strain habit plane. In this particular transformation it worked out in such a way that the magnitude of the inhomogeneous shear was rather sensitive to the dilatation parameter. He did not feel very happy about the magnitude of the dilatation parameter but he did not think Dr Crocker's argument against it was particularly convincing – Dr Crocker suggested that if there were no volume change one should not use a dilatation parameter. In steels, however, one sometimes used a dilatation parameter of opposite sign to that of the overall volume change.

His other point on the zirconium and titanium transformations concerned the question of the {334} or {344} habit planes: it was not always possible to distinguish these two clearly by measuring the habit plane itself. The distinction depended on the direction of the displacement in the shape deformation, and one had to measure the shape deformation before one was sure which type of martensite one was discussing. The direction of displacement lay on different zones in the two cases.

Referring back to Mr Garwood's paper and the question of whether one could have a bainitic transformation when both components of a solid solution ought to be diffusing or moving at comparable rates, the paper of his own to which reference had been made had been written some years ago. In the light of Mr Garwood's experimental evidence one had to think about these things again, but he was not convinced by the theoretical argument presented in Mr Garwood's paper that the diffusional movements were of a different kind from those which should destroy the correspondence. He thought that the reason for having bainitic transformation in substitutional alloys, if this was really what happened, must simply be that one component could diffuse much faster than another.

There was one other matter about which he was not very clear in the work on non-ferrous bainitic transformations. The thermodynamics said that an α-phase was being precipitated or formed from the β-phase, but what experimental evidence was there of the actual compositions of the phase formed in this part of the reaction? He would like to hear anything that could be said about this.

Mr Garwood said, concerning the change in composition, that there was certainly a shift in the lines of the Debye–Scherrer X-ray spectra of the β-phase as the α precipitated from solid solution. It was difficult to be very precise about the magnitude of the change because, as Dr Christian was probably aware, this precipitation reaction was accompanied by considerable line broadening.

Dr L. Kaufman said, on the point relating to compositional changes, that he had done experiments with β-brass where one could cycle many times through the $\alpha \rightarrow \beta$ reaction without changing the reaction temperatures. It seemed to him that if there were substantial changes in the composition of the product and daughter phases, there would be a gradual increase, in this case, of the M_s temperature as one went through many cycles; although chemical analysis of the daughter phase had not been attempted at the time, shifts had never been observed.

Mr Garwood pointed out that the remarks he had just made concerned the isothermal reaction which took place well above the M_s temperature. He was not talking about the martensite reaction at all, but agreed that there was no evidence of a compositional change during thermal cycling in the sub-zero temperature range of the martensite reaction. In this connexion he said that he had worked recently on the effect of precipitating bainite plates at 180°C on the martensite transformation of the residual β. Those present might be aware that Pops and Massalski had shown that the martensite transformation in brass took place in two stages. There was an M_s for thermoelastic martensite and a burst effect at a lower temperature. The M_s temperatures previously reported corresponded to the burst effect at the lower temperature. It had been found that tempering a material containing 41·3%Zn at 180°C, to cause bainitic precipitation to start, had the effect of changing the emphasis of the martensite transformation from the burst at the lower temperature to the major volume fraction transforming at the higher thermoelastic M_s point, identified by Pops and Massalski. Clearly bainitic precipitation activated nuclei for the martensite transformation.

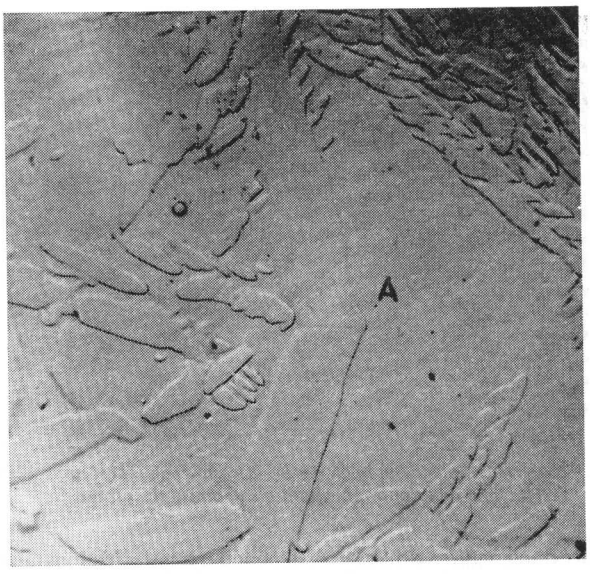

V *40·5%Zn alloy heat treated at 450°C for 8 s, showing internal striations in the plate pair revealed on etching; these relate to the inhomogeneous shear component; carbon/platinum replica* ×3750

WRITTEN CONTRIBUTIONS

Dr Armitage wrote that a greater range of applications for titanium alloys might be achieved by obtaining bainitic microstructures. In particular, a favourable combination of strength and ductility might be produced.

Figure *M* showed a selection of microstructures formed in adjacent regions of a specimen from the near-eutectoid alloy *G* during quenching from the β-range; martensite (M), a bainitic structure (B), and pearlite were produced.

Figure *N* showed the same alloy after further aging at 550°C when the microstructure contained tempered martensite (TM), bainite (B), and pearlite (P).

The presence of both pearlitic and bainitic structures after

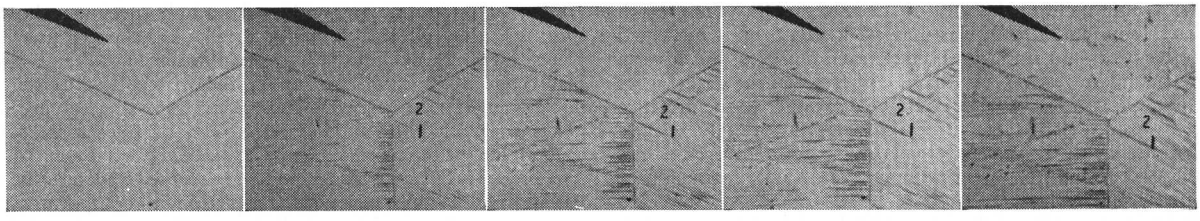

t *t*+26s *t*+46s *t*+66s *t*+110s

W *Still cine sequence of 44·1%Zn specimen heat treated at 390°C on hot stage microscope; rod 1 shows a linear change of length with time*

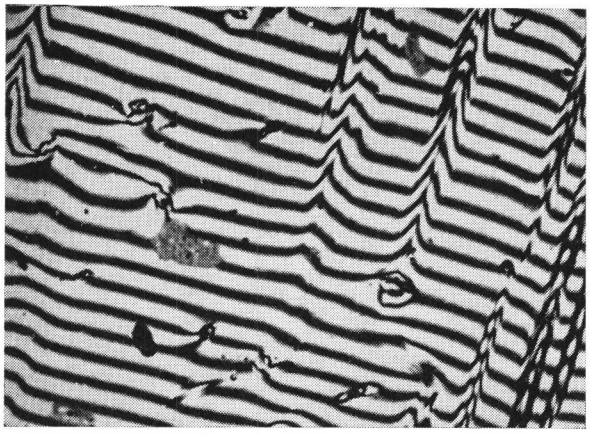

X *Interference photograph of 44·1%Zn specimen, heat treated at 520°C for 6 min, confirming multiple nature of the surface tilt*

quenching suggested that the corresponding transformations must proceed at very short transformation times in this alloy.

To obtain a more uniform microstructure the alloy was subsequently quenched from the β-range to isothermal transformation temperatures between 550° and 750°C. Figure *O* gave an example of the microstructure after 2 h transformation at 630°C, which showed colonies of a bainitically nucleated structure that had probably coarsened during isothermal holding. This transformation took place above the M_s of the alloy, so martensite was not produced. Pearlite was present only at the original β-grain boundaries.

Future investigations could be aimed at assaying the mechanical properties produced by bainitic microstructures in several binary titanium alloys. Further additions of isomorphous β-stabilizing elements might prove useful towards suppressing the pearlite transformation so that a more homogeneous microstructure could be obtained.

Dr A. Bar-Or and **Dr A. Rosen** (Israeli Atomic Energy Commission) wrote that the purpose of their present study of the martensitic transformation in uranium–chromium alloys was to investigate whether the nucleation of the needles was a heterogeneous process and which heterogeneities acted as nuclei. They were interested to learn to what extent the slow rate of growth of the individual martensite needles should be attributed to transformation stresses, as suggested by Holden,[19] or to the complexity of atom adjustments as suggested by Lomer.[20]

To examine the effect of various inhomogenieties on the nucleation of martensite, uranium–chromium alloy specimens containing impurities, β–β grain boundaries, cracks, and a rim of α-grains were prepared. The α-rim was introduced by means of isothermal transformation from the β-phase at 620°C.[21,22]

The different specimens were quenched from β, polished and heat treated under vacuum at temperatures below 110°C, and subsequently examined under the microscope for the appearance of martensitic needles. After measuring the length and width of the needles the specimens were sealed again in quartz capsules under vacuum and further heat treated. In this way the growth of each individual needle was measured. The needles nucleated almost entirely on impurities, cracks, and pinholes, but not on grain boundaries or on the α-rim. The fact that the grains were not potential nucleation sites could be due either to the presence of a chromium-rich layer on the α–β boundary or to the relative unimportance of the interfacial energy barrier compared to the barrier due to the stress field generated during the formation of the martensite nucleus.

Preliminary results of the longitudinal and transverse growth of the martensite needles as a function of the time and temperature of the isothermal heat treatment were shown in Figures *P* and *Q*. Both the length and width of the needles seemed to increase linearly with time.

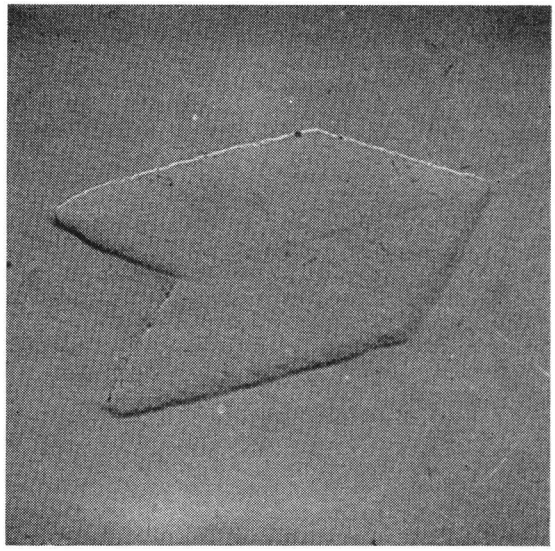

Y *44·1%Zn alloy heat treated at 260°C for 20 h, showing angular rods of α with an apparent twin relationship about the common interface; carbon/platinum replica* ×16000

Using the well known Arrhenius equation the values of Q_e=12300 cal/mole and Q_w=11700 cal/mole were calculated, where Q_e and Q_w were the activation energies for longitudinal and transverse growth, respectively.

Further experimental and theoretical studies were being conducted on the interpretation of the activation energies, which could lead to a better understanding of this very interesting martensitic transformation.

Mr P. E. J. Flewitt and **Mr J. M. Towner** (Battersea College of Technology) wrote that it was interesting to note the agreement between the results reported by Professor Hehemann and those shown in Figure 5 of Mr Garwood's paper,[23] showing the variation of the rod to plate transition temperature with composition. However, his results for lower zinc contents were open to discussion. Their own results indicated that the rate of reaction in bulk material was very high, particularly for the lower zinc alloys (Figure *R*). Thus below ~40 wt-% the incubation period was less than 1 s, and it would be difficult to determine experimentally the upper limit for the formation of the plates. It would seem justifiable to obtain the upper limit of this transition by linear extrapolation, to lower zinc content, of the B_s in Figure 5 of Mr Garwood's paper. Further, the variation of the tentatively designated B_s temperature with zinc content seemed to indicate that the order/disorder transition had little effect on the plate to rod change. With decreasing solute content the degree of order of the metastable β' decreased leading to a decrease in the ordering temperature. If this order/disorder change were to have an effect it would act in the reverse sense to that reported.

Electron microscopy on replicas from bulk specimens showed the nucleation of small α-plates ahead of the other growing plates (Figure *S*). It could be assumed that ahead of the growing plate edge a stress was set up in the matrix leading to the nucleation of new α-plates, subsequent growth allowing the plates to link. This 'sympathetic' form of nucleation could account for the observed tendency of the plates to cluster.

A single surface analysis technique[24] was used to determine the variation of the habit plane of the α-plates with composition and temperature. Compositions studied were 40·5 wt-%Zn at 200°C and 350°C, also 43·0 wt-%Zn at 230°C. The loci of all possible poles of the habit planes were collected into a unit stereographic

triangle shown in Figure *T*. Within experimental error, the habit plane was the same for the compositions and temperatures examined. The pole values fell close to the $\{2.11.12\}_\beta$ previously reported for the 41·3%Zn alloy.[25]

Figure *U* showed the apparently crystallographic degeneration of the α-plates in the mixed product region just below B_s. In this region plates of α formed initially, but rods could be subsequently nucleated to form a mixed product. Figure *V*, region *A*, showed a plate formed in this range exhibiting internal striations revealed by etching; this internal structure was assumed to form as a result of the second inhomogeneous shear required for plate formation. The directions exhibited by this internal structure corresponded closely to those observed in the degeneration of the plate shown in Figure *U*. Therefore the possibility existed that the rods of α could nucleate on the interface of the α-plates as well as independently in the surrounding β'. In the former case, since these rods would tend to be more stable than the plates, the nucleation of the rods led to the degeneration of the initial plates.

Surface relief was found to be present on the formation of α-rods which was consistent with a structure of two adjacent regions separated by a midrib. The rods then developed a multiple relief with a characteristic feather pattern. The development of this multiple relief was shown by the sequence of photographs in Figure *W* taken from a cine-film obtained using a hot stage microscope. The multiple nature of the surface relief was supported by the interferogram Figure *X*

Two further points might be of interest. Firstly thermal etch-pits were observed on a specimen of 44·1%Zn giving a regular array of pits at the α/β interface, suggesting the presence of a semi-coherent interface for rods. Secondly, with higher zinc content the α-rods showed flat facets, especially at lower temperatures. Figure *Y* showed two such rods exhibiting an apparent twin relationship about the common interface.

REFERENCES

1. R. F. Mehl and O. T. Marzke: *Trans. AIME*, 1931, **93,** 123.
2. O. T. Marzke: *ibid.*, 1933, **104,** 64–68.
3. W. K. Armitage: This report.
4. A. B. Greninger: *Trans. AIME*, 1939, **133,** 204–227.
5. P. R. Swann and H. Warlimont: *Acta Met.*, 1963, **11,** 511–527.
6. D. S. Lieberman *et al.*: *J. Appl. Phys.*, 1955, **26,** 473–484.
7. W. Jolley and D. Hull: *J. Inst. Met.*, 1964, **92,** 129–135.
8. J. K. Mackenzie and J. S. Bowles: *Acta Met.*, 1957, **5,** 137–149.
9. A. J. Williams *et al.*: *ibid.*, 1954, **2,** 117–128.
10. P. Gaunt and J. W. Christian: *ibid.*, 1959, **7,** 534–543.
11. L. Kaufman: *Acta Met.*, 1959, **7,** 575.
12. V. C. Huang: *J. Japan. Inst. Met.*, 1963, **227,** 429.
13. J. C. Jamieson: *Science*, 1963, **140,** 72.
14. F. P. Bundy: 'Irreversible effects of high pressure and high temperature on the properties of materials', ed. L. Kaufman; Special Technical Publication No. 374, 1965, Philadelphia, ASTM.
15. L. Kaufman: in 'Energetics in metallurgical phenomena', ed. W. Mueller; 1965, Denver, Colorado, University of Denver.
16. A. Jayaraman *et al.*: *Phys. Rev.*, 1963, **131,** 644–649.
17. A. G. Crocker: Ph.D. Thesis, Sheffield University, 1959.
18. W. M. Lomer: 'The mechanism of phase transformations in metals', 337; 1956, London, Institute of metals.
19. A. N. Holden: *Acta Met.*, 1953, **1,** 617–623.
20. W. M. Lomer: 'The mechanism of phase transformations in metals', 243–253; 1956, Institute of Metals.
21. A. Bar-Or and P. Wynblatt: *J. Inst. Met.*, 1963, **92,** 183–184.
22. A. Bar-Or *et al.*: *Trans. AIME.* To be published.
23. R. D. Garwood: This report.
24. J. S. Bowles: *Trans. AIME*, 1951, **191,** 44.
25. R. D. Garwood: *J. Inst. Met.*, 1954–55, **83,** 64–68.

High-carbon bainitic steels

K. J. Irvine, B.Sc., Ph.D., and F. B. Pickering, A.Met., F.I.M.

SYNOPSIS

An investigation of bainitic steels over the carbon range from 0·1 to 1·0% has been carried out. For this purpose, a ½%Mo–B base composition was adopted, which gave bainitic structures in the air-cooled condition over the full range of carbon contents. An additional series of steels was used based on 1%Cr–½%Mo–B to obtain lower transformation temperatures in the bainitic range. The isothermal and continuous cooling transformation characteristics have been determined and also the tempering characteristics of the air-cooled structures. Mechanical properties have been determined in the air-cooled condition and after tempering at temperatures up to 700°C. The bainitic structures were studied by optical and electron microscopes. From this work, it has been possible to relate the structural features to the mechanical properties and to suggest reasons for the strength of the bainite. It has also been possible to describe the main features of the bainite transformation, which are essentially the same over the whole range of carbon contents, and to distinguish between the upper and lower bainite structures. It has been shown that a steel with the composition 0·5/0·6%C, 1%Cr, ½%Mo, 0·003%B is capable of giving a tensile strength of 90–100 tons/in² in large section sizes in the air-cooled condition. 2610

INTRODUCTION

The physical metallurgy of low-carbon bainitic steels has been fully described in a series of papers published over the last few years.[1–6] This work led to the development of commercial steels in which the carbon content was limited to obtain satisfactory weldability. This necessarily limited the maximum tensile strength to about 70 tons/in². For applications where weldability is not essential it is possible to use higher carbon contents and hence obtain greater strength. The object of the work described in this paper was to investigate the physical metallurgy of higher carbon bainitic steels which could then serve as the basis for the development of commercial steels.

In order to ensure that a bainitic structure was developed, steels of the ½%Mo–B type were used. Such steels retard the pro-eutectoid ferrite transformation considerably more than the bainite transformation and hence allow bainitic structures to be obtained over a wide range of cooling rates. Since the alloy content is low, the martensitic hardenability is not very high, which means a bainitic structure is obtained even at rapid cooling rates. In low-carbon steels, boron is extremely effective as an alloying element to increase bainitic hardenability. The effect of boron is known to decrease at higher carbon contents,[7] and for steels approximating to eutectoid composition it is doubtful whether boron is necessary. However, to maintain a consistent series boron was included in all the experimental steels examined. To explore the full range of transformation temperature, some alloy addition is required to depress the transformation temperature. The scope for alloy addition is limited, however, because of the associated increase in martensitic hardenability and hence the addition was restricted to 1%Cr. Consequently, two series of steels with carbon contents varying between 0·1 and 1% were made using two base compositions of ½%Mo–B and 1%Cr–½%Mo–B. With these steels it was possible to compare with previous work published on bainitic steels and to extend the study to include the full range of carbon content and transformation temperature. Details of the analyses of these steels are given in Table I. All the steels were rolled to ¾in diameter before examination. The physical metallurgy aspects covered included the determination of the isothermal transformation, continuous cooling transformation, and tempering characteristics. The mechanical properties were determined in the air-cooled and tempered conditions with a detailed study of the microstructures in these conditions. From this it has been possible to relate the mechanical properties to the structural changes and also to put forward an explanation of the mechanism of the bainite transformation and suggest reasons for the strength of bainite.

TRANSFORMATION TEMPERATURES

The transformation temperatures on cooling were determined for both series of steels using samples cooled at a rate equivalent to the air cooling rate of ¾in diameter bar from an austenitizing temperature of Ac_3+30°C. From these results a temperature was obtained representing 50% transformation. The effect of variation in carbon and the 1%Cr addition is shown in Figure 1.

Dr Irvine is Metallurgical Research Manager and Mr Pickering is Head of the Physical Metallurgy Section at the Research and Development Department of The United Steel Companies Ltd. (MG/Conf/84/65). UDC No. 669.15–194: 669.112.227.33

TABLE I Analyses of steels

Steel no.	Analysis, % C	Mn	Si	Cr	Mo	Sol. B	
1	0·10	0·52	0·11	—	0·54	0·0033	½%Mo–B series
2	0·20	0·59	0·22	—	0·52	0·0033	
3	0·32	0·46	0·22	—	0·53	0·0034	
4	0·41	0·62	0·23	—	0·54	0·0034	
5	0·61	0·53	0·36	—	0·53	0·0023	
6	0·83	0·50	0·35	—	0·53	0·0014	
7	0·93	0·63	0·29	—	0·49	0·0042	
8	1·06	0·48	0·34	—	0·54	0·0017	
9	0·12	0·52	0·27	1·08	0·54	0·0038	1%Cr–½%Mo–B series
10	0·22	0·57	0·21	1·05	0·51	0·0038	
11	0·32	0·63	0·29	1·03	0·49	0·0040	
12	0·42	0·59	0·28	0·99	0·52	0·0024	
13	0·53	0·50	0·15	1·30	0·55	0·0012	
14	0·65	0·50	0·46	1·01	0·52	0·0032	
15	0·82	0·51	0·41	1·18	0·52	0·0034	
16	0·96	0·66	0·37	1·00	0·53	0·0040	
17	1·04	0·65	0·57	1·08	0·50	0·0030	

In the ½%Mo–B steel series the transformation temperature is depressed with increasing carbon up to 0·7%C and in the 1%Cr–½%Mo–B steel series up to 0·5%C. Above these carbon contents the transformation temperature increases again, since in the higher carbon steels there is undissolved carbide after the austenitizing treatment which nucleates for the pearlite transformation and hence raises the transformation temperature. To obtain complete solution of the carbides, it is necessary to use higher austentitzing temperatures as below:

½%Mo–B steels		1%Cr–½%Mo–B steels	
0·41%C	800°C	0·53%C	850°C
0·61%C	800°C	0·65%C	950°C
0·83%C	900°C	0·82%C	1000°C
1·06%C	950°C	1·04%C	1050°C

If these austenitizing temperatures are used the transformation temperatures of the higher carbon steels are also depressed in line with the trend shown for lower carbon steels.

It can be seen that not only is there a marked effect of increasing carbon depressing the transformation temperature, but that this effect is greater in the 1%Cr series of steels.

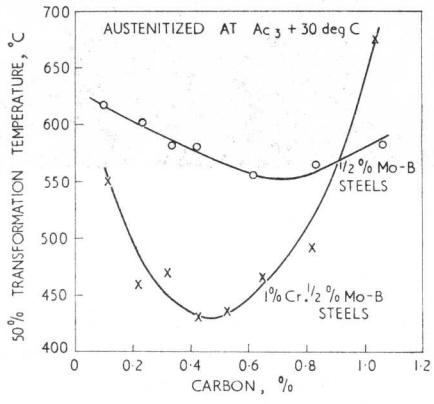

1 *Effect of carbon content on transformation temperatures during air-cooling ¾in diameter bar*

MICROSTRUCTURES OF AIR-COOLED BARS

The microstructures of the air-cooled ¾in diameter bars are shown in Figures 2 and 3, the higher carbon steels in both series being austenitized at temperatures which virtually dissolved all the carbides. Figure 2 shows that in the ½%Mo–B steels all the structures were bainite, and with increasing carbon content the amount of dark etching high-carbon bainite increased. Above 0·6%C the structures showed a typical high-carbon upper bainite structure. With increasing carbon content the acicularity of the structures also increased due to the depression of the transformation temperature.

Figure 3 shows that the 1%Cr–½%Mo–B steels had more acicular bainitic structures than the lower alloy steels, due to the increased alloy content lowering the transformation temperature. Up to 0·4%C the structures showed bainites of increasing carbon content and decreasing transformation temperature, but above 0·4%C the martensitic hardenability increased so much that in air-cooled ¾in diameter bar martensite began to be formed together with bainite. The amount of martensite increased with increasing carbon content until in the 0·8%C steel the structure was almost fully martensitic. The M_S temperature of the 1%C steel was so low that there were considerable amounts of retained austenite together with the martensite. The presence of martensite in the higher carbon, higher alloy steels correlates with the decreased proof stress values obtained in the tensile tests, which will be discussed later.

These results show the increase of martensitic hardenability with carbon content, especially at the higher alloy contents. This means that there must be a critical balance of the composition between alloy and carbon content to maintain a fully bainitic structure.

TENSILE PROPERTIES OF AIR-COOLED HIGH-CARBON BAINITIC STRUCTURES

Because of the pronounced effect of the austenitizing temperature on the transformation characteristics due to the undissolved carbides in the higher carbon steels, the tensile properties of the higher carbon steels were determined from both the Ac_3+ 30°C and from a higher austenitizing temperature which virtually dissolved all the carbides. These results are summarized in Figure 4.

Figure 4*a* shows that in the ½%Mo–B steels the increase in carbon content caused a linear increase in tensile strength and 0·2% proof stress, but a slight decrease in proof ratio from 0·75 to 0·65–0·70. Increasing carbon also produced a decrease in the tensile ductility. All the structures were fully bainitic even at the highest carbon content. Increasing the normalizing temperature to dissolve all the carbides in the higher carbon steels caused a slight increase in strength and 0·2% proof stress, amounting to about 5 tons/in² on the 0·2% proof stress in the 1%C steel. This indicated that there was not much carbide undissolved at the lower normalizing temperature, even in the 1·06%C steel in this series.

Figure 4*b* shows that in the 1%Cr–½%Mo–B steels an increase in carbon content up to 0·6% caused an increase in tensile strength and 0·2% proof stress, but above 0·6% the tensile strength and proof stress decreased. This was the result of the structure in the higher carbon steels consisting of martensite and some retained austenite. Up to 0·4%C, there was no

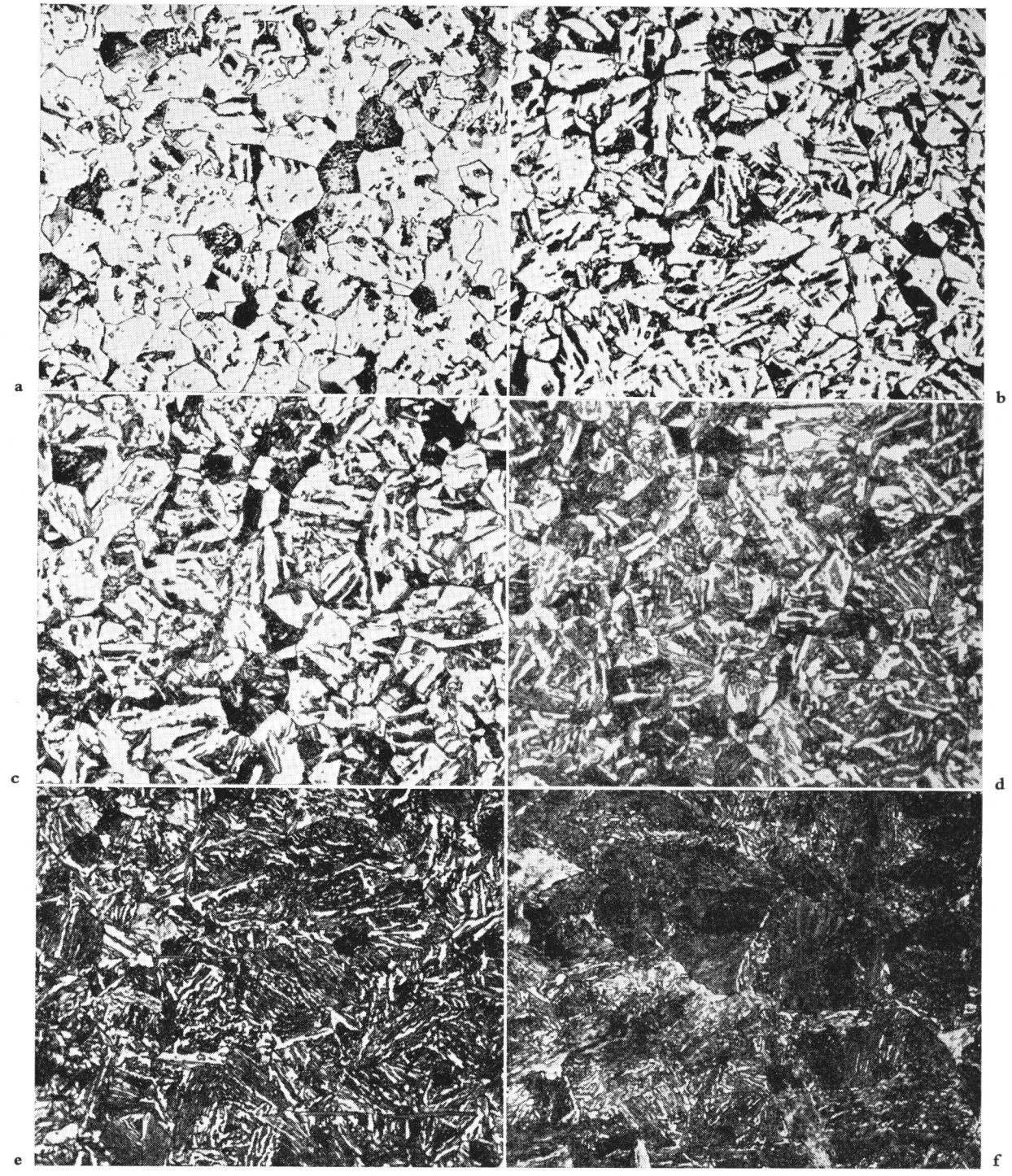

a 0·20%C; **b** 0·32%C; **c** 0·41%C; **d** 0·61%C; **e** 0·83%C; **f** 1·06%C

2 *Microstructures of ½%Mo–B steels normalized as ¾in diameter bar* ×750

advantage to be gained by using a higher normalizing temperature because there were no undissolved carbides, but between 0·4% and 0·7%C the higher normalizing temperature produced an increase in tensile strength and 0·2% proof stress. At the highest carbon contents, however, the tensile strength and proof stress markedly decreased after the higher normalizing temperatures, because the greater effective carbon content of the steel caused more retained austenite. Increasing carbon content at the lower normalizing temperatures caused very little change in the proof ratio, which was 0·58–0·65. In general,

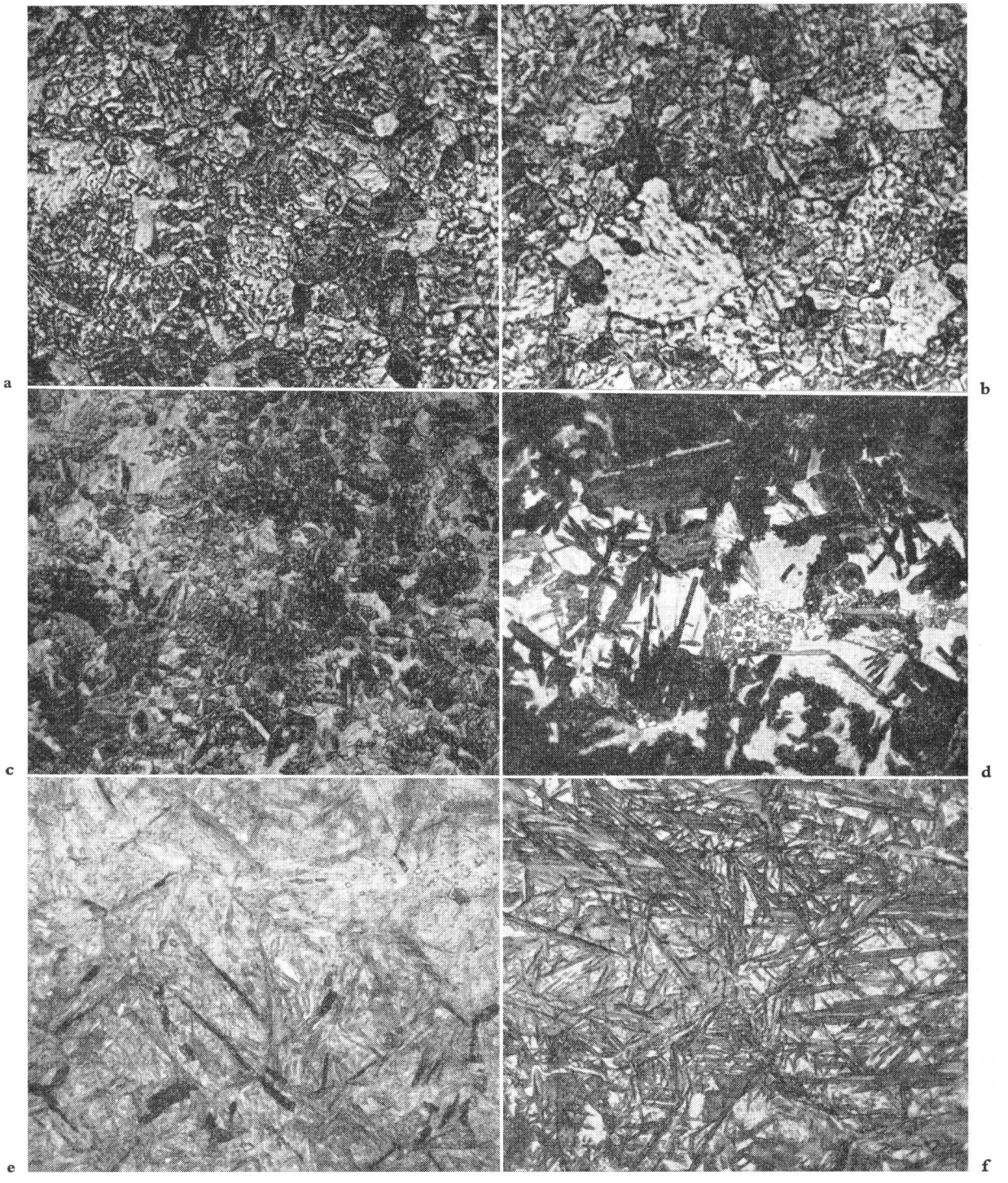

a 0·22%C; **b** 0·32%C; **c** 0·42%C; **d** 0·65%C; **e** 0·82%C; **f** 1·04%C

3 *Microstructures of 1%Cr–½%Mo–B steels normalized as ¾in diameter bar* ×750

however, the higher normalizing temperature gave a higher proof ratio. The tensile ductility decreased with increasing carbon content but there was no systematic trend of higher normalizing temperatures.

From a comparison of the tensile properties of the ½%Mo–B and 1%Cr–½%Mo–B steels, it can be seen that the 1%Cr–½%Mo–B steels had much increased tensile strengths and, except at the highest carbon contents, much increased proof

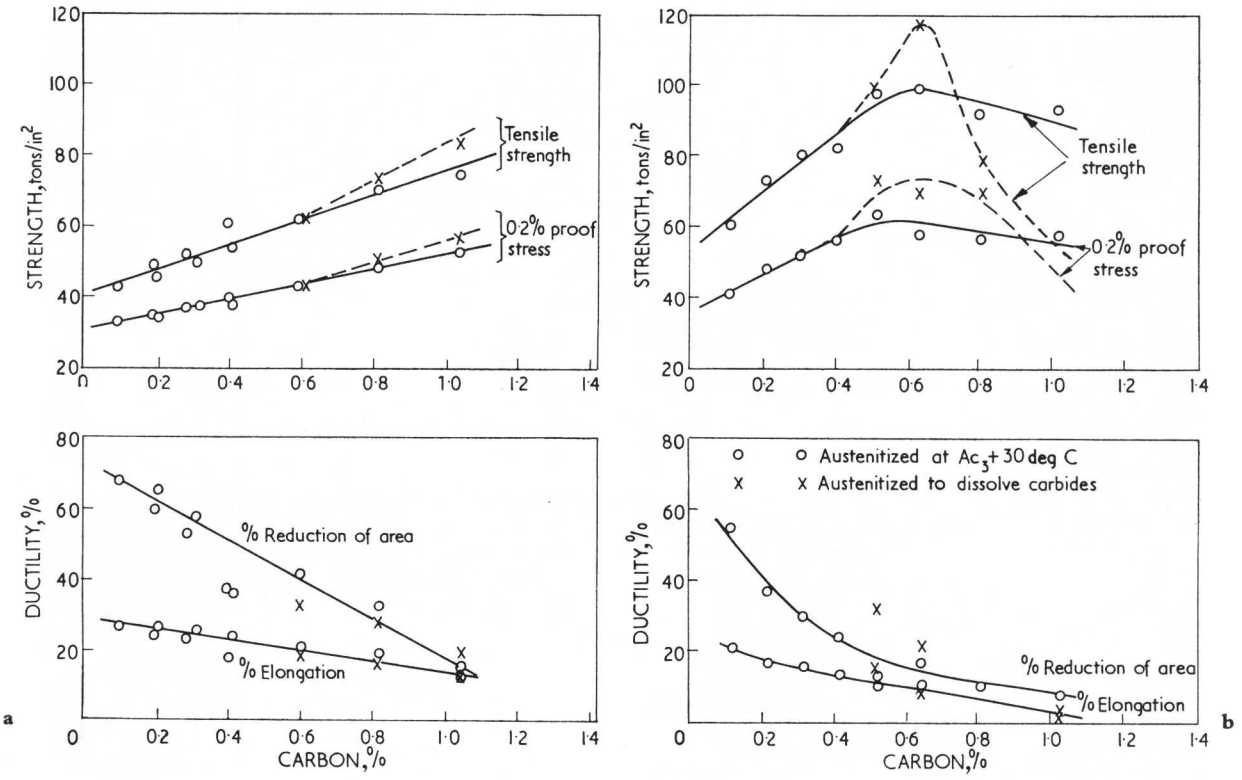

a ½%Mo–B steels; **b** 1%Cr–½%Mo–B steels.

4 *Effect of carbon content on the mechanical properties*

stress values compared with the ½%Mo–B steels. This is mainly due to the lower transformation temperatures. The increased tensile strengths were only achieved at the expense of a considerable reduction in ductility. If, however, the ductilities obtained at a given tensile strength are compared, it can be seen that the 1%Cr–½%Mo–B steels had rather better ductilities than the ½%Mo–B steels. In both cases the structures being compared were fully bainitic. This comparison is given below (*see* Table at foot of page).

The main reason for the improved ductilities in the 1%Cr–½%Mo–B steels at comparable strength levels is the lower carbon contents at which such strengths can be achieved.

The comparison between the two series of steels is also illustrated by the hardness values. Figure 5 shows the hardness values of these steels obtained after normalizing at the higher temperatures compared with the typical curve for the effect of carbon on the martensitic hardness. In the 1%Cr–½%Mo–B steels, the hardness approaches the martensitic hardness level at 0·8%C but falls off again as retained austenite is introduced into the structure at higher carbon contents.

TEMPERING CHARACTERISTICS

The tempering characteristics were determined after normalizing from the temperature which dissolved all carbides; consequently the initial hardness levels were those shown in Figure 5. The tempering curves of the two series of steels are shown in Figures 6 and 7. All of the ½%Mo–B steels had bainitic structures and tempering at temperatures up to 500°C caused little or no softening from the initial hardness values. Tempering temperatures above 500°C caused progressive softening to occur. In the 1%Cr–½%Mo–B steels structures were bainitic up to 0·6%C and on tempering there was a gradual decrease of hardness during tempering at temperatures up to 500°C; the effect being more pronounced with increasing initial hardness. This effect was due to precipitation of carbon from the bainite and also to growth of the existing carbide particles. At tempering temperatures above 500°C much more rapid softening occurred due to

Tensile strength, tons/in²	RA, %		Elongation, %		Carbon, %	
	1% Cr–½% Mo–B	½% Mo–B	1% Cr–½% Mo–B	½% Mo–B	1% Cr–½% Mo–B	½% Mo–B
60	53	41	22	20	0·10	0·58
70	37	25	17	15	0·23	0·87
80	26	13	13	11	0·36	1·16

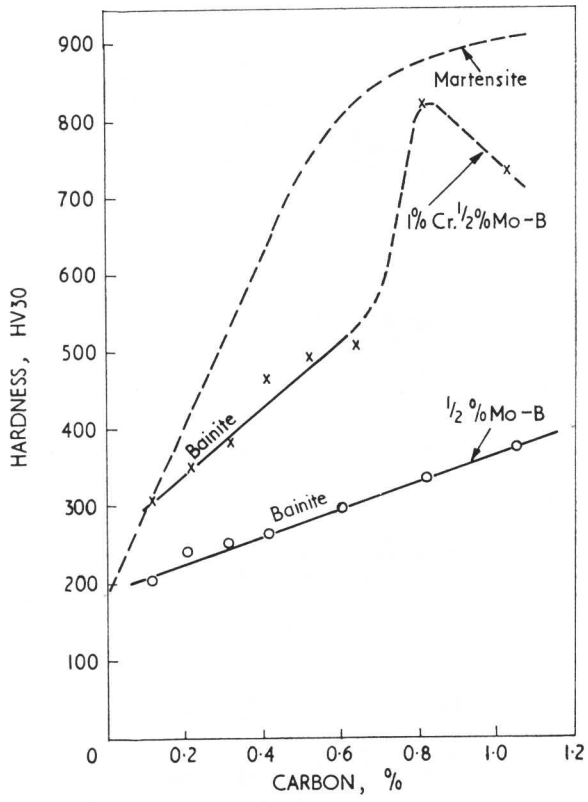

5 *Effect of carbon content on hardness*

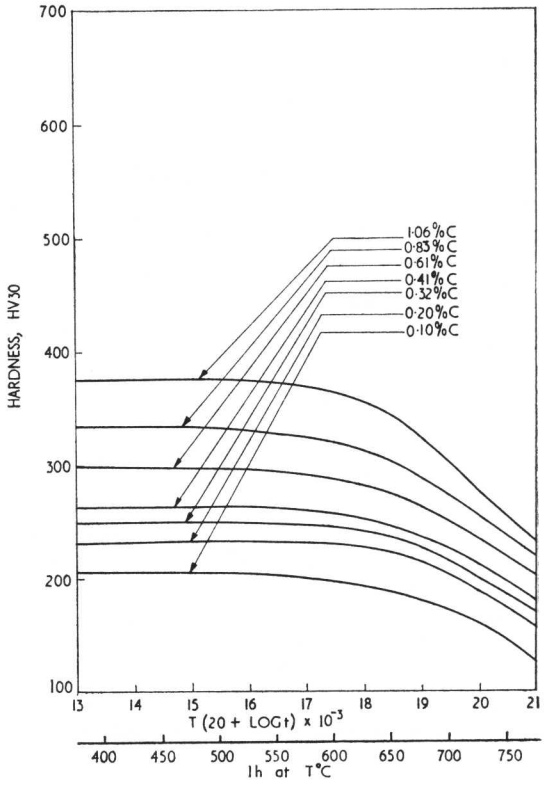

6 *Tempering characteristics of ½%Mo–B steels*

the growth of the carbide particles and possibly, in the later stages of tempering, to some ferrite grain growth. The 0·8%C and 1%C steels had very different tempering characteristics because of their different initial structures. The 0·8%C steel was initially martensite and showed progressive softening from the high initial hardness level with increasing tempering temperature. The 1%C steel was initially martensite and austenite and showed an increase of hardness, due to the decomposition of austenite, at low tempering temperatures up to 300°C, and then subsequent softening at higher tempering temperatures. In the higher tempering temperature range these two high-carbon steels fell into line with the trend shown by the lower carbon bainitic steels. It is clear that carbon has the controlling influence on the hardness, both in the initial bainitic condition and after tempering. This relationship is shown for both series of steels in Figure 8.

MECHANICAL PROPERTIES OF TEMPERED STEELS

Tensile properties were determined on both series of steels after tempering for 1 h at temperatures between 400°C and 700°C. The normalizing temperature used was Ac_3+30°C. The results are summarized in Figures 9 and 10 as a function both of carbon content and tempering temperature. The effect of carbon was to increase linearly the tensile strength and 0·2% proof stress values, but this effect became less marked at high tempering temperatures. Tempering at low temperatures of 400°–500°C did not affect the tensile strength very much but increased the proof stress due to the relief of internal stresses. The effect was to increase proof stress to tensile strength ratio. This was particularly evident in the 1%Cr–½%Mo–B steel which

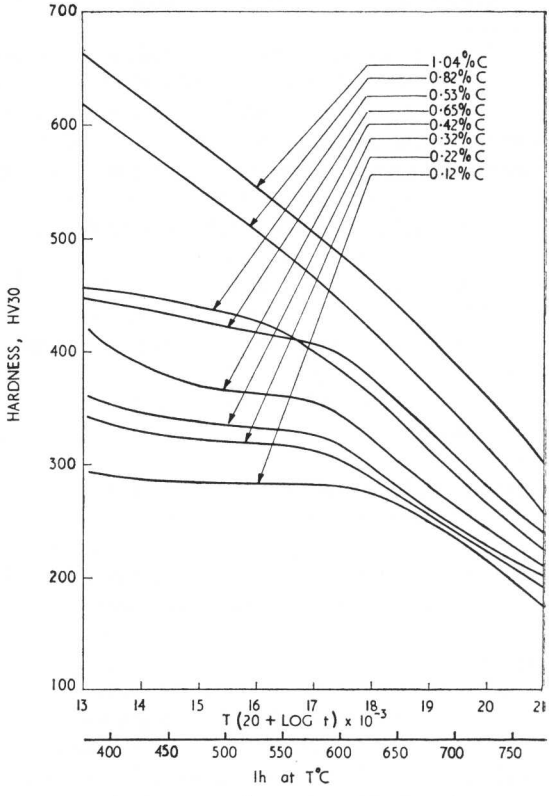

7 *Tempering characteristics of 1%Cr–½%Mo–B steels*

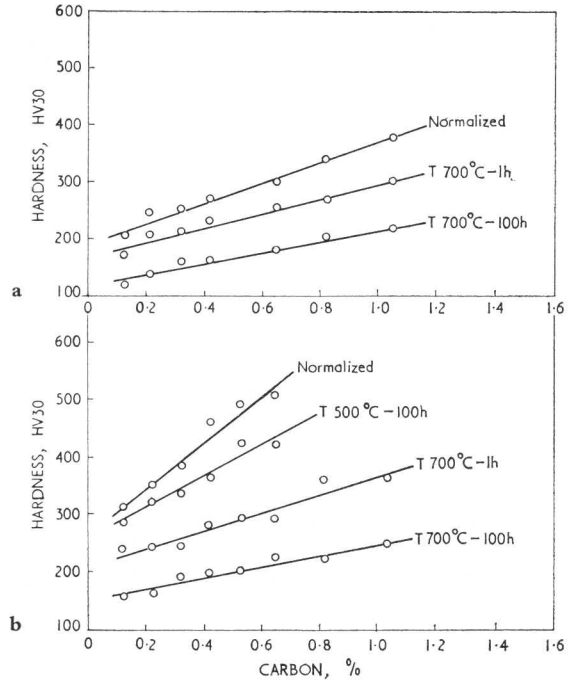

a ½%Mo–B steels; **b** 1%Cr–½%Mo–B steels.

8 *Effect of carbon content on hardness after tempering*

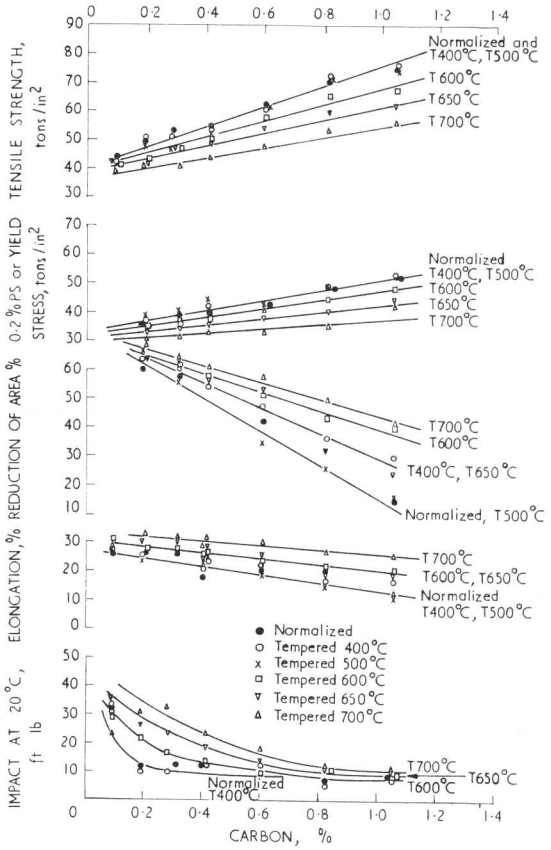

9 *Effect of carbon content and tempering temperature on mechanical properties of ½%Mo–B steels*

transformed at lower temperatures than the ½%Mo–B steel. The effect of increasing the tempering temperature on the ductility was in general to increase both the reduction of area and elongation.

The effect of tempering on the impact resistance can also be seen from Figures 9 and 10. In each series of steels the impact resistance in the normalized condition decreased with increasing carbon content and tempering up to 500°C produced little improvement. Increasing tempering temperatures up to 700°C improved the impact properties of the lower carbon steels, i.e. up to 0·6%C, but had little effect on the higher carbon steels. In general, the effect of tempering was more pronounced on the 1%Cr–½%Mo–B steels, and at the 0·5%C level these steels had considerably better impact properties than the ½%Mo–B steels. This is presumably due to the lower initial transformation temperature in the 1%Cr–½%Mo–B steels, which produces a lower temperature bainitic structure having inherently better impact resistance.

MECHANICAL PROPERTY RELATIONSHIPS

When considering the possible applications for high-carbon bainitic steels, it is necessary to know how the properties compare with those obtainable from other structures, particularly tempered martensite which is the most widely used high-strength structure. In the first place, it is necessary to have a satisfactory ratio of 0·2% proof stress to tensile strength, preferably of the order of 0·75. Figure 11 shows the relationship between 0·2% proof stress and tensile strength for these high-carbon bainitic steels. It will be seen that in the air-cooled condition the proof ratio is low, decreasing to roughly 0·6. It need hardly be mentioned that the proof ratio of a martensitic steel would also be low in the untempered condition because of the considerable amount of internal stress in the structure. After tempering the proof ratios of the high-carbon bainitic steels are raised to the satisfactory level of 0·75–0·8.

Another interesting comparison is the ductility obtainable at a given strength level. This relationship is shown for the high-carbon bainitic steels in Figure 11 and, for comparison, a line is drawn representing the relationship found by Janitsky and Baeyertz[14] for quenched and tempered steels. It will be seen that in the air-cooled condition the ductility values of the high-carbon bainitic steels are lower than the Janitsky–Baeyertz relationship and are only partially raised to this level by tempering. There is a difference between the ½%Mo–B and the 1%Cr–½%Mo–B steels in this respect. The 1%Cr–½%Mo–B steels are raised very close to this line, whereas the ½%Mo–B steels have a lower ductility. This is more apparent in the reduction of area figures than the elongation, and appears to be due to the relative carbon content of these steels. The 1%Cr–½%Mo–B steels, because of the higher alloy content, can achieve a given tensile level at a lower carbon content than the ½%Mo–B steels and, therefore, are closer in carbon content to the Janitsky–Baeyertz steels, which were predominantly 0·35–0·45%C. In this connexion, reference should be made to previously published work on low-carbon bainitic steels[2] containing 0·08–0·14%C. These steels had appreciably better ductility than the Janitsky–Baeyertz relationship. It appears, therefore, that while bainitic

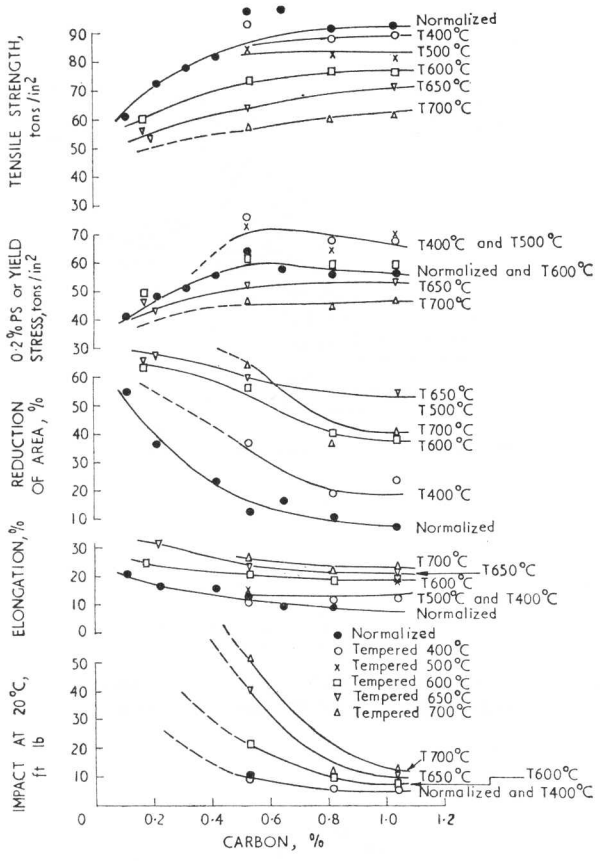

10 *Effect of carbon content and tempering temperature on mechanical properties of 1%Cr–½%Mo–B steels*

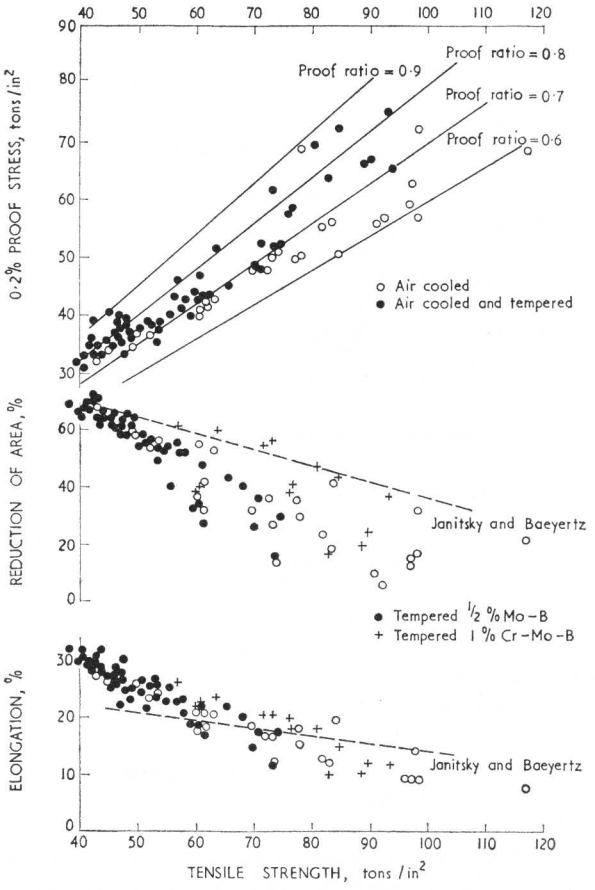

11 *Mechanical property relationships in high-carbon bainitic steels*

structures in general have similar ductility to tempered martensite at equivalent tensile strength levels, this is influenced by carbon content, the higher carbon content steels having lower ductility.

Another important property is impact resistance, which is very sensitive to structural variations, and it is clear that the impact values shown in Figures 9 and 10 for high-carbon bainitic steels are lower than those which can be obtained from quenched and tempered steel. It is also clear that the impact resistance would need to be better before these steels would find much commercial application. The important point to remember here is that the work described in this paper has been directed more at understanding the bainitic structure than developing a commercial steel. Within the limitation of the bainitic structure it is possible to make appreciable changes in composition which can improve the impact resistance without losing strength. Work of this type is currently in hand and is giving encouraging results.

ISOTHERMAL TRANSFORMATION CHARACTERISTICS

Isothermal transformation diagrams were determined after austenitizing at Ac_3+30°C for the lower carbon steels or at the higher temperatures mentioned previously which are necessary to dissolve the carbide in the higher carbon steels.

½% Mo-B steels

A selection of 0% transformation lines from the isothermal diagrams is shown in Figure 12. The following comments can be made:

(i) all the steels showed a bay in the diagram due to molybdenum

(ii) with increasing carbon content, the temperature of the nose of the ferrite and/or pearlite reactions decreased; the depression of the ferrite *C* curve was related to the effect of carbon lowering the Ac_3 temperature, while carbon also depressed the B_S temperature and consequently lowered the temperature of the nose of the bainite *C* curve

(iii) the effect of carbon content on the period of induction at the nose of the ferrite/pearlite and bainite reactions, is shown in Figure 14; the proeutectoid ferrite reaction was retarded by increasing the carbon content up to 0·5%, but above 0·5% the reaction was accelerated; in the hypereutectic steels containing more than 0·8%C the nose of the diagram was controlled by the pearlite reaction and was accelerated by increasing carbon due to some remaining undissolved carbides which nucleated for the formation of pearlite; the effect of increasing the carbon content on the period of induction at the

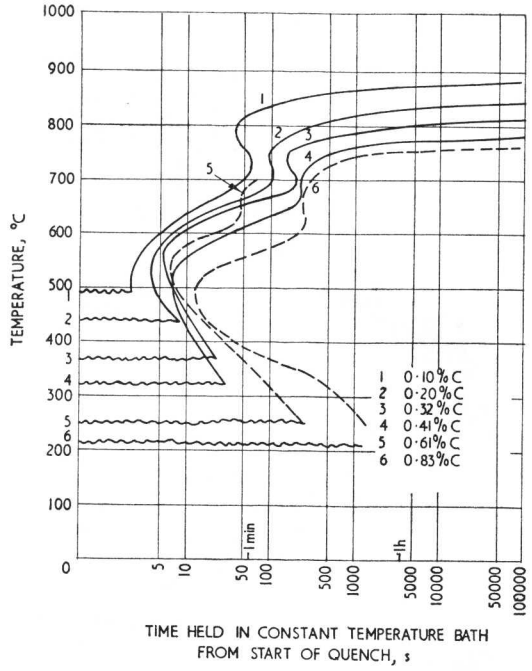

12 *Effect of carbon content on the isothermal transformation diagrams of ½%Mo–B steels; 0% curves only are shown*

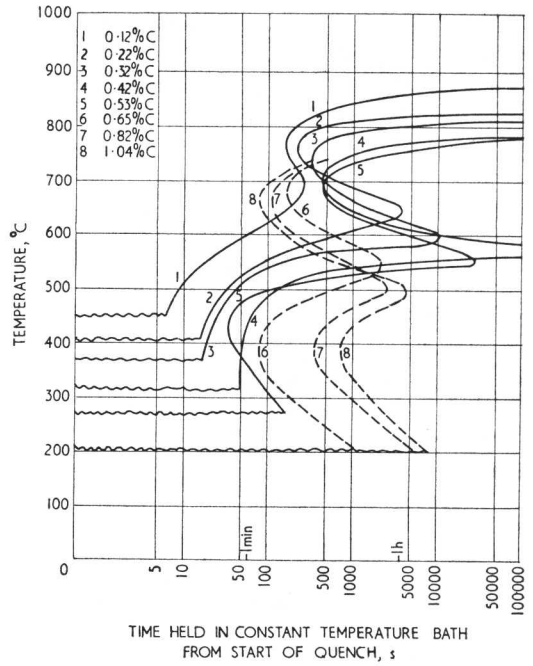

13 *Effect of carbon content on the isothermal transformation diagrams of 1%Cr–½%Mo–B steels; 0% curves only are shown*

nose of the bainite reaction caused a progressive retardation of the reaction

(iv) with increasing carbon content, the ferrite and pearlite reactions were always retarded considerably more than the bainite reaction, which means that the bainitic structure would be formed during continuous cooling, over a wide range of cooling rates; also, because the bainite reaction was not greatly retarded, martensite would not be formed, except at very rapid cooling rates

(v) a point of interest was the change in the rate of the bainite reaction below 350°C in steels containing more than 0·6%C; this gave a rather more rapid reaction than would be anticipated from an extrapolation of the kinetics of the upper bainite reaction to lower temperatures; this has been observed by other workers,[8,9] and is attributed to the change from upper to lower bainite; it will be seen to correlate with the microstructural differences between upper and lower bainite.

1%Cr-½%Mo-B steels

The 0% transformation lines from the isothermal diagrams are shown in Figure 13. The following comments can be made:

(i) all the steels showed a marked bay between the ferrite/pearlite and the bainite reaction; this was more marked than in the ½%Mo–B steels due to the presence of 1%Cr

(ii) increasing carbon lowered the Ac_3 temperature and, therefore, also lowered the temperature of the nose of the ferrite and/or pearlite reactions

(iii) increasing the carbon content slightly depressed the nose of the bainite reaction, the effect being even less than in the ½%Mo–B steels

(iv) increasing the carbon content progressively retarded the proeutectoid ferrite reaction (Figure 14); when the

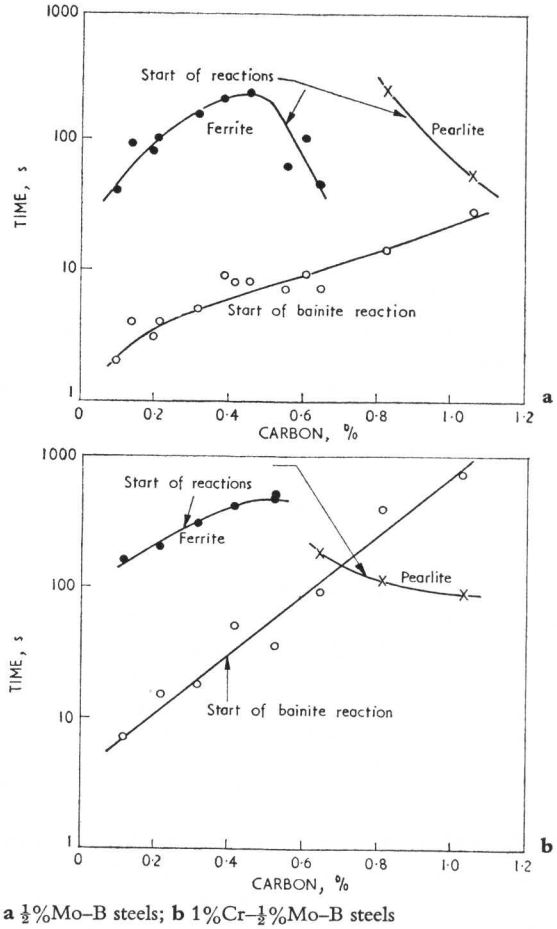

a ½%Mo–B steels; **b** 1%Cr–½%Mo–B steels

14 *Effect of carbon content on the start of ferrite, pearlite, and bainite reactions*

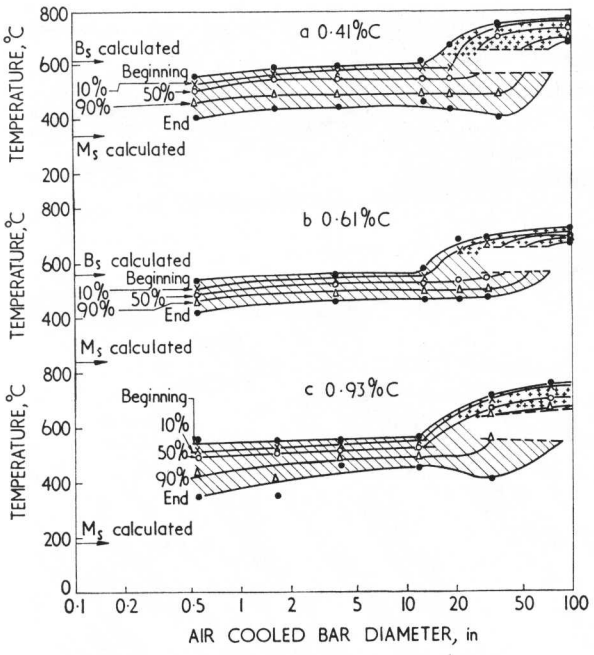

15 *Continuous cooling transformation diagrams of ½%Mo–B steels with varying carbon contents*

carbon content exceeded 0·6% the steel became hypereutectoid and increasing carbon content accelerated the pearlite reaction due to some remaining undissolved carbides nucleating the pearlite reaction; the bainite reaction was again progressively retarded by increasing carbon content

(v) perhaps the most significant difference between the ½%Mo–B and 1%Cr–½%Mo–B steels was the fact that in the more highly alloyed steel and at the higher carbon contents the bainite reaction was retarded more than the pearlite reaction; during continuous cooling, therefore, at rates of cooling fast enough to avoid the pearlite reaction, martensite would be formed instead of bainite.

CONTINUOUS COOLING TRANSFORMATION CHARACTERISTICS

Continuous cooling diagrams were determined for a number of these steels using an austenitizing temperature of 950°C. These diagrams are shown in Figures 15 and 16.

½% Mo-B steels

The steels exhibited high bainitic hardenability with fully bainitic structures being developed at a cooling rate equivalent to air-cooled 12in diameter bar. Figure 15 shows that there was little variation with increasing carbon content up to 0·9%. When the carbon increased above 1%, however, undissolved carbides nucleated the pearlite reaction and restricted the range for bainite transformation to about 5in diameter air-cooled. The martensitic hardenability was low so that even in air-cooled ½in diameter bar martensite was not formed. Consequently, with steels up to 0·9%C, bainitic structures can be achieved at air-cooling rates over a wide range of section sizes. Since the transformation temperature does not vary greatly within this range, the strength obtainable should be consistent with different section sizes.

1%Cr-½%Mo-B steels

Up to about 0·6%C, the bainitic hardenability is high. In fact the 0·6%C steel should be capable of forming a bainitic structure during air-cooling sections up to 25in diameter. The martensitic hardenability in these steels is low so that martensite would not form in air-cooled ½in diameter bar. Consequently, the range of section sizes which will form a bainitic structure is very wide. Above 0·6%C, the steel becomes hypereutectoid and the maximum size for bainitic structures during air-cooling is reduced to 2–5in diameter. At the same time the martensitic hardenability is higher and martensite will form in air-cooled 1in diameter bar. Since this is a very restricted range for achieving bainitic structures it can be seen that the maximum carbon content which should be used at this level of alloy content is 0·6%C.

Some further continuous cooling transformation diagrams were determined on these higher carbon steels using an austenitizing temperature of 1050°C. This was to dissolve carbides more completely and prevent the pearlite reaction being nucleated and accelerated. The cooling range for bainite transformation was extended to larger air-cooled bar diameters but the higher austenitizing temperature also had the effect of increasing the martensitic hardenability. It was still concluded, therefore, that for the greatest range of application the carbon content should be limited to 0·6%.

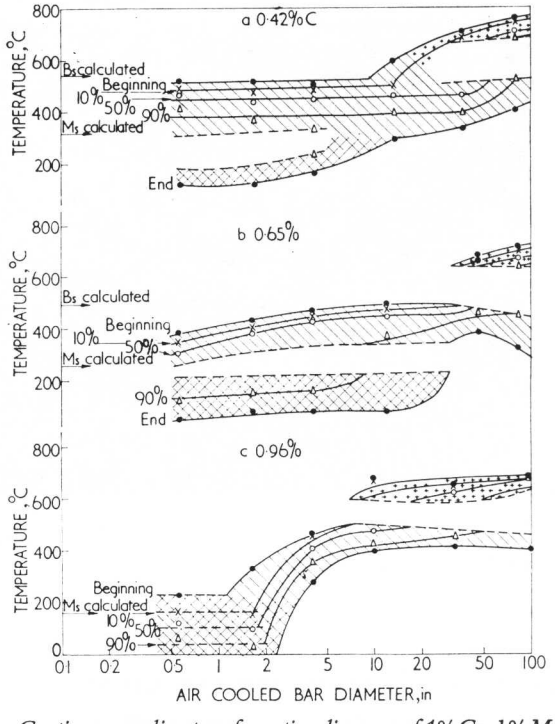

16 *Continuous cooling transformation diagrams of 1%Cr–½%Mo–B steels with varying carbon contents*

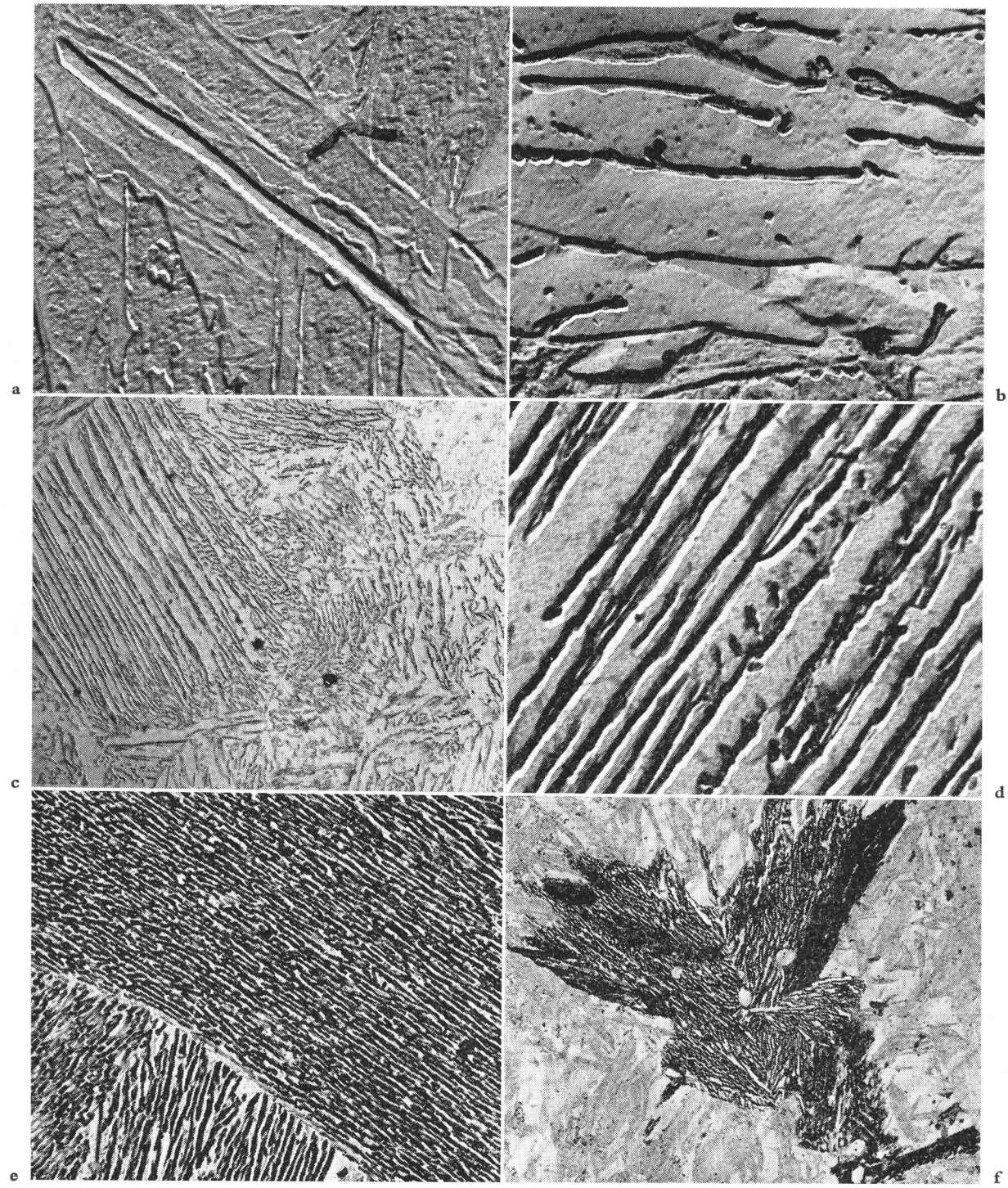

a start of transformation at 550°C, 0·2%C ×15 000
b fully transformed structure at 550°C, 0·2%C ×15 000
c side-by-side nucleation of bainite needles, 0·6%C ×3 000
d fully transformed structure at 500°C, 0·6%C ×15 000
e fully transformed structure at 400°C, 1·06%C ×15 000
f wedge shaped upper bainite patches after partial transformation at 400°C, 1·06%C ×3 000

17 *Electron micrographs of upper bainite*

FORMATION OF THE BAINITIC STRUCTURES

While the morphology of low-carbon bainite is now fairly well established,[3,5] the structure of higher carbon bainite is not so well understood, and in fact the electron microstructures of high-carbon bainite are not so easy to interpret.

The two types of low-carbon bainite are typified as upper

and lower bainite respectively. Both are nucleated by a small plate or needle of ferrite formed by a shear mechanism from the austenite (Figure 17*a*). The strain produced by the shear transformation activates many adjacent nuclei so that bainitic ferrite plates form side by side.

Upper bainite

In upper bainite, the diffusion rate of carbon is sufficiently high for carbon to diffuse away in front of the bainitic ferrite plates into the surrounding austenite, which becomes considerably enriched in carbon. This eventually tends to stop the lateral growth of the bainitic ferrite needles. At lower transformation temperatures carbon diffuses less rapidly and so a carbon concentration is built up more quickly in the austenite. This means that the growth of the ferrite plates is hindered and that thinner bainite needles will be produced at the lower transformation temperatures. Also, due to the rapid side-by-side nucleation of needles, the carbon-enriched austenite is trapped between the ferrite needles. Carbide eventually forms from this austenite as films lying between the bainitic ferrite needles and parallel to their longitudinal direction (see Figure 17*b*). This carbide may well form directly from the austenite and an examination of the orientation relationship between the carbide and ferrite in upper bainite suggests that, at least in low-carbon steels, this relationship appears to be derived from a mutual relationship between the carbide and the austenite and the ferrite and austenite.

Basically, the upper bainite reaction is the same in high-carbon steels as in low-carbon steel, but certain modifications are introduced by the higher carbon content of the initial austenite. The initial nucleus may still be a bainitic ferrite plate, or it may be a carbide needle precipitated directly from the austenite, particularly in the higher carbon content steels or at the lower transformation temperatures in the upper bainite range. Even if a carbide plate occurs first, the carbon concentration gradient set up around it appears to enable ferrite plates to be nucleated adjacent to the carbide.

In 0·6%C steels at temperatures near to B_S, the high initial carbon content of the austenite causes the carbon enrichment around these ferrite plates rapidly to stop the growth of the ferrite, but the shear strains in the higher carbon steel still give many side-by-side nucleated needles, despite the greater difficulty in producing a suitable low-carbon nucleus (Figure 17*c*). The entrapped austenite regions then transform to carbide films between the bainitic ferrite needles (Figure 17*d*), which are thinner than in lower carbon steels.

The higher the carbon content and the lower the transformation temperature, the more rapidly is the carbon concentration necessary to stop the lateral growth of the ferrite needles produced, with the result that the ferrite needles become thinner and have discontinuous films of carbide (formed from the entrapped austenite) between them. This structure in certain orientations can have a very lamellar appearance (Figure 17*e*). The first needle formed will have had greater opportunity for lengthwise growth so that successive needles on either side of it will be shorter, and this gives the characteristic wedge or spear shape to the bainite patches (Figure 17*f*). It seems, however, that the lower the transformation temperature and the higher the carbon content in the upper bainite range, the more difficult becomes the co-operative side-by-side nucleation of the bainitic ferrite. Eventually, a temperature is reached at which the carbon has such a slow rate of diffusion that it can no longer diffuse away adequately in front of the bainitic ferrite, and the carbon content in the ferrite is too high for the reaction to continue. Upper bainite cannot then form and is replaced by lower bainite.

Lower bainite

In lower bainite the only way in which the carbon content of the bainitic ferrite can be reduced sufficiently to allow the reaction to continue is by precipitation of carbides within the bainitic ferrite plates. These carbides form as small plates orientated with respect to the longitudinal axis of the needles. This is a very characteristic feature of lower bainite and may be due to precipitation occurring on twins in the bainitic ferrite. An examination of the orientation relationship between carbide and ferrite in lower bainite, using thin-foil electron microscopy, confirms that the cementite precipitates directly from the ferrite. The orientation relationship appears to be that for the precipitation of cementite from high-carbon martensite (i.e. twinned martensite), and is as found by Pitsch and Schrader.[10]

The lower bainite reaction is the same for all carbon contents, except that more carbides are precipitated within the ferrite needles in the higher carbon steels. Typical microstructures are shown in Figure 18. The first needles formed in a 0·6%C steel (Figure 18*a*) contain carbides, which are also seen with their characteristic morphology in the more fully transformed structure (Figure 18*b*). Exactly the same type of structure is observed at 1%C (Figure 18*c*).

One feature of these microstructures is that the lower bainite needles in high-carbon steels are often thicker than the upper bainite needles formed at slightly higher temperature. This is analogous to martensite needles which are frequently observed to be wider than lower bainite needles. The reason is probably related to the increased driving force for the reaction at lower temperatures which causes greater growth of the bainitic ferrite needles, despite the fact that it is supersaturated with carbon.

An interesting effect of carbon content on the temperature at which upper bainite is replaced by lower bainite was observed. In 0·1%C steels, this temperature has been shown to be approximately 450°C[1] but the current work shows that when the carbon content increases to 0·4% this temperature is increased to about 550°C. With still further increase in carbon content the temperature of the change from upper to lower bainite rapidly decreases to 350°C, as observed by a number of workers using high-carbon steels.[11–14] These effects can be explained in terms of the general mechanism of bainite formation already discussed. The temperature at which upper bainite is replaced by lower bainite is that at which the rate of carbon diffusion is so slow that carbon can no longer diffuse away in front of the growing bainitic ferrite. As the initial carbon content of the austenite is increased, however, this point will be reached at an increasing temperature, since with a smaller carbon gradient in the austenite a higher temperature is necessary to give an equivalent diffusion rate of

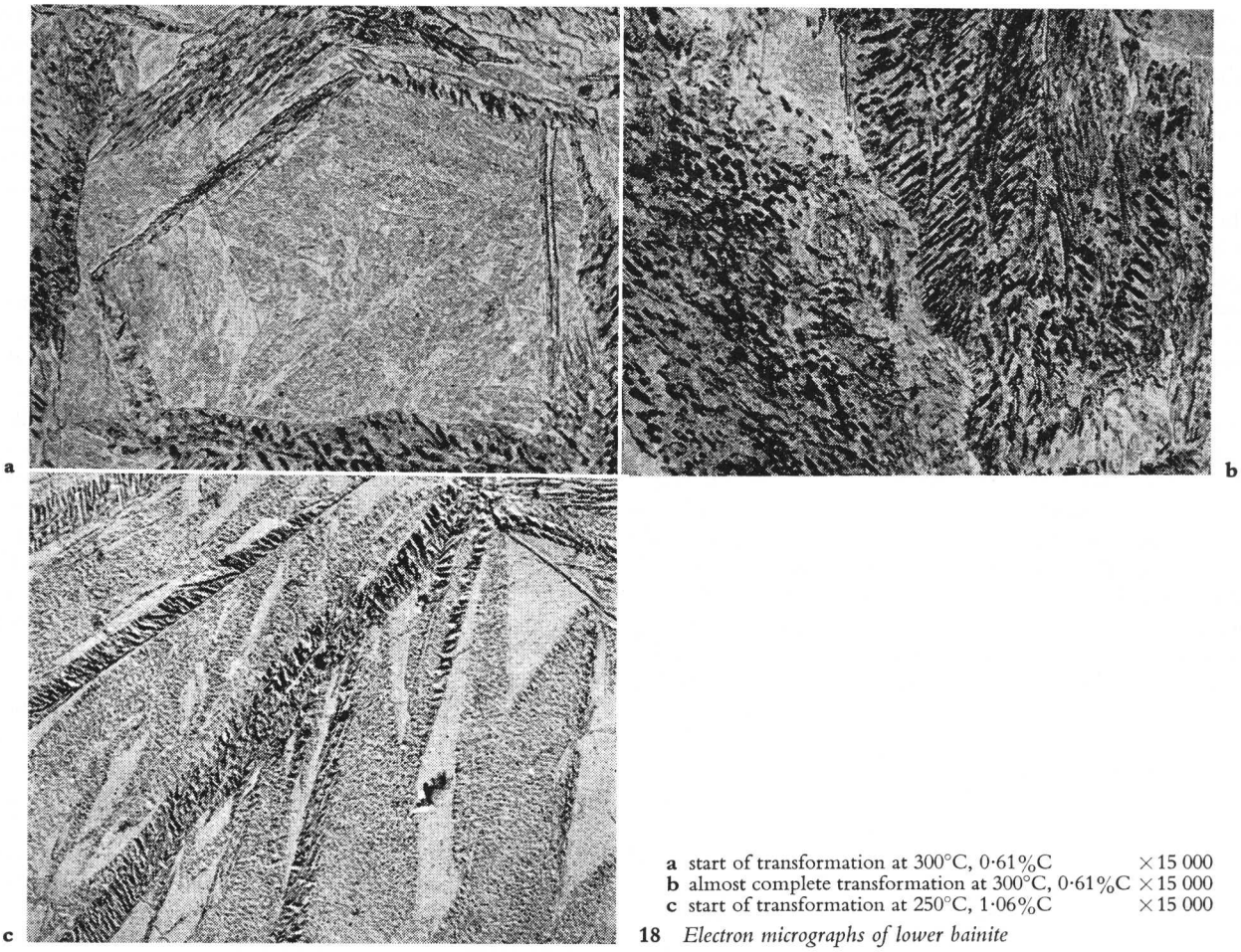

a start of transformation at 300°C, 0·61%C ×15 000
b almost complete transformation at 300°C, 0·61%C ×15 000
c start of transformation at 250°C, 1·06%C ×15 000

18 *Electron micrographs of lower bainite*

carbon away from the interface. In a steel containing more than 0·5%C, the extrapolated Ac_m line intersects the curve denoting the upper temperature limit of lower bainite formation. When this occurs, any steel containing more than 0·5%C is effectively hypereutectoid below about 550°C, and primary carbide will precipitate directly from the austenite; this is, of course, the mode of carbide precipitation in upper bainite. The only change in this mode of transformation occurs at the very much lower temperature of 350°C when the rate of carbide precipitation becomes very slow and kinetically the formation of supersaturated ferrite and the precipitation of carbide from it becomes the more favourable process; this is the mode of carbide precipitation in lower bainite. Consequently, with all steels containing more than 0·5%C, the temperature for the change from upper to lower bainite is roughly 350°C.

There is also interest in the bainitic ferrite itself, which can best be studied by thin-film electron microscopy. Some work on upper and lower bainite has been carried out, predominantly on lower carbon steels where it is believed that the properties of the bainitic ferrite are more important in controlling the properties of the bainitic structure. It was shown that there is a small misorientation between neighbouring bainitic ferrite grains. The boundaries between them were, in general, composed of dislocation arrays (Figure 19*a*). These boundaries have been observed to obstruct dislocation movement and, therefore, will contribute to the strength of the structure. With decreasing transformation there is an increase in the dislocation density of the bainitic ferrite. Figure 19*a* shows a low-carbon steel transformed at 550°C, whereas Figure 19*b* is the same steel transformed at 450°C. The bainitic ferrite plates are smaller and there is a much higher dislocation density. This will also contribute to the strength of the structure. Lower bainite seems to have a higher dislocation density than upper bainite formed at the same temperature, possibly because of the carbides precipitated from the ferrite.

STRENGTH OF BAINITE

There are a number of possible reasons for the strength of bainite.

a Fine bainitic ferrite grain size

It has been shown in previous work on the bainitic structure[3,5] that as the transformation temperature decreases the bainitic ferrite grain size becomes smaller. It has also been shown that this is directly related to the increasing strength of the structure. The grain size becomes smaller with decreasing transformation temperature because there is a more

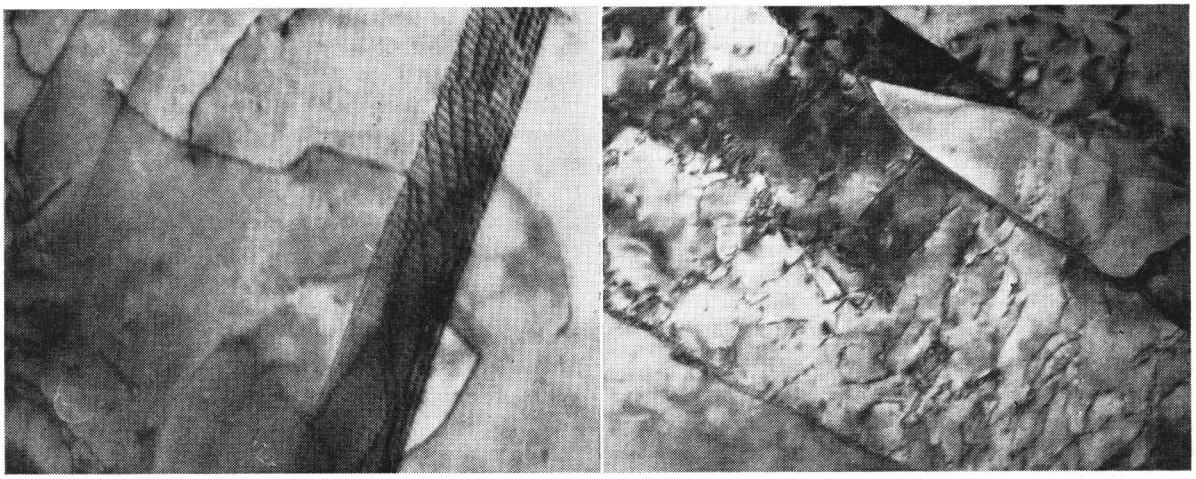

a transformed at 550°C ×100 000 **b** transformed at 450°C ×80 000

19 *Thin-foil micrographs of upper bainite in a lower carbon steel*

rapid build-up of a carbon-enriched layer at the interface due to the slower rate of diffusion of carbon with decreasing transformation temperature. It seems clear that this effect will become more pronounced in the higher carbon bainitic steels, but it becomes extremely difficult to make a reliable grain size measurement. There has been some speculation about the effect of the low-angle boundaries between the bainitic ferrite grains but this work has shown that there is sufficient misorientation across them to act as obstacles to dislocation movement.

b Carbide dispersion

It is also known that as the transformation temperature decreases the carbide particles become finer, more numerous, and more evenly dispersed. This produces a greater dispersion hardening effect. A good relationship has been shown between the number of carbide particles and the strength.[5] In these higher carbon bainitic steels the increasing carbon content will increase the number of carbide particles and will, therefore, add to the strength.

c Internal stress

As the transformation temperature is decreased the dilation occurring during the transformation increases and this must lead to greater internal stress in the bainitic ferrite. This will contribute to increased strength and it is interesting to note from the mechanical properties obtained that it also results in anomalously low proof stress values. The proof stress tensile strength ratio decreases with decreasing transformation temperature and can only be restored by tempering to remove internal stresses.

d Dislocation density

It has been shown that all bainites, even those formed at high temperatures, have a greater dislocation density than polygonal ferrite. This must also contribute to the strength of the structure. These dislocations are generated by the strains associated with the shear transformation. These strains also cause the adjacent austenite to be deformed and so contain a higher dislocation density than annealed austenite. During the growth of the bainitic ferrite plates into this deformed austenite some dislocations will be inherited. It is possible that the carbides also help to generate a high dislocation density. This could be a contributory cause of the higher strength in high-carbon bainitic structures.

e Carbon dissolved in bainitic ferrite

It has been shown[11] that with decreasing transformation temperature more carbon is left dissolved in the bainitic ferrite. This produces solid-solution strengthening and it is possible that there is some association of the interstitial carbon atoms and the dislocations in the ferrite.

It is difficult to evaluate the contribution of the above factors to the strength of the bainitic structure and, in fact, the contribution of each changes according to the carbon content and the transformation temperature. However, it is possible to make some generalizations about this.

In low-carbon steels, the important factors at high transformation temperatures are the fine bainitic ferrite grain size and the dislocation density of the bainitic ferrite. As the transformation temperature is decreased carbide particle dispersion hardening becomes more important, but the effect is limited by the low carbon content.

In high-carbon steels, the carbide dispersion hardening effect is much more important throughout the transformation temperature range. At high transformation temperatures the bainitic ferrite plate size is, of necessity, small and the ferrite will contain dislocations. However, the strength obtainable is not greatly different from the strength of a 1%C steel transformed at 600°C to pearlite. In this case, a hardness of 470 HV30 can be obtained, due almost entirely to dispersion hardening. It is concluded, therefore, that the major contribution to the strength of a high-carbon bainitic structure transformed at a high temperature is the dispersion hardening effect of the carbide. Support for this viewpoint is given by

the fact that little or no softening occurs on tempering up to 500°C and that softening above this temperature is associated with spheroidization and coalescence of the carbides.

At lower transformation temperatures (below 450°C) the hardness increases appreciably and this is not apparently due to any major change in the amount of the dispersed carbide. It is concluded that the increase in hardness results from the enforced solid solution of carbon in the bainitic ferrite. Support for this viewpoint is given by the fact that softening does occur at low tempering temperatures as carbon is precipitated from solution to form carbides.

DESIGN OF HIGH-CARBON BAINITIC STEELS

Before deciding the factors which are important in designing high-carbon bainitic steel, it is useful to consider where such a steel might find commercial application. It has been shown previously that low-carbon bainitic steels can offer an attractive combination of strength and weldability, but the low carbon content limits the maximum strength to approximately 70 tons/in^2. In fact, after tempering to give stress relief to ensure high proof stress values, the strength level drops to perhaps 55 tons/in^2. Also, the wide range of strength obtainable from a quenched and tempered steel must be taken into account. The application of such steels are limited only by the martensitic hardenability, which may prevent the strength being obtained in large section sizes, and the stresses associated with the quenching treatment, which may cause distortion and cracking. It seems clear, therefore, that the scope for high-carbon bainitic steel is in a strength range from 70 tons/in^2 up to the maximum obtainable. Such steels are likely to be used where this strength level is required in large section sizes and where distortion would be harmful. They are also likely to be preferred where the high carbon content, and hence the large number of carbide particles, gives enhanced wear resistance. It should also be remembered that the alloy content is low and consequently the cost should be low. Typical of the application envisaged is a large die block or a back-up roll. It is realistic to conclude, however, that these will be rather special and limited applications.

If the requirement is a strength range from 70 to, say, 110 tons/in^2, then it is possible to suggest the composition range necessary. The ½%Mo–B steels described in this paper represent the lowest alloy content that can be used. With this base composition it is possible to obtain a strength of 80 tons/in^2 at about 0·8%C. In such a steel the transformation temperature is still relatively high and higher strength can be obtained if the transformation temperature is depressed by an alloy addition. Up to 1%Cr can be added with a consequent increase in tensile strength to 100 tons/in^2.

As the alloy content is raised, however, the martensitic hardenability is increased so that martensite is formed at air-cooling rates in small diameter sections. The choice of alloying element and its amount is, therefore, important. What is required is an alloying element which will depress the B_S temperature but not markedly retard the bainite transformation. This would give the lowest transformation temperature and, therefore, the highest strength, and allow the carbon content to be reduced to give the highest ductility. The martensitic hardenability would be low and hence the structures should be completely bainitic. The effect of elements on the depression of the B_S are known from the work of Steven and Haynes[15] and also from previous work on low-carbon bainitic steels.[2] Manganese and chromium are most effective, followed by molybdenum and nickel. Little is known about the effect of these elements on the retardation of the bainite reaction at different carbon contents, but from general hardenability considerations it is possible that manganese has less effect than chromium and would, therefore, be preferred. The difference is likely to be slight, however, and therefore the work on 1%Cr–½%Mo–B steels provides a good guide to the effects. It seems clear that the maximum permissible alloy addition to the ½%Mo–B base is about 1%, and that the optimum carbon range is 0·5/0·6%. With this type of steel, i.e. 0·5–0·6%C, 1%Cr, ½%Mo, 0·003%B, the following properties can be obtained in the normalized condition: tensile strength 90–100 tons/in^2, 0·2% PS 55–65 tons/in^2, RA 20–25%, and elongation 10–15%.

These properties can then be improved by tempering, which improves the 0·2% PS to tensile strength ratio and also improves the ductility and impact resistance. There is obviously scope for further development work within the limits stated on the actual composition to give specific combinations of mechanical properties.

CONCLUSIONS

This work has extended the study of bainitic steels up to 1%C. The following conclusions can be drawn.

1. With a base composition of ½%Mo–B, it is possible to obtain fully bainitic structures over the complete range of carbon contents from 0·1 to 1·0%. These bainitic structures are obtained at air-cooling rates over a wide range of section sizes from ½in to 12in diameter.

2. These high-carbon ½%Mo–B steels give tensile strengths in the normalized condition from 40 tons/in^2 at the 0·1%C level to 83 tons/in^2 at the 1%C level. There is little decrease in strength with tempering up to 500°C but the strength decreases when the tempering temperature is increased to 600°–700°C.

3. When the alloy content is increased by the addition of 1%Cr the bainitic transformation is depressed. Up to 0·6%C the bainitic hardenability is very high and bainitic structures are formed at air-cooling rates in sections up to 25in diameter, but the martensitic hardenability is still low. When the carbon content is increased above 0·6% the martensitic hardenability is increased and the hypereutectoid nature of the steel accelerates the pearlitic transformation. Consequently, the bainitic transformation is restricted to air-cooled section sizes of 2–5in diameter.

4. The tensile strength level of the 1%Cr–½%Mo–B steel in the normalized condition ranges from 60 tons/in^2 at the 0·1%C level to 100 tons/in^2 at the 0·6%C level. This was further increased to 116 tons/in^2 by using a normalizing temperature sufficiently high to dissolve all carbides. At higher carbon contents, the strength decreased due to the presence of martensite and some retained austenite.

5. The most likely requirement is for a tensile strength of 80–100 tons/in^2 with high bainitic hardenability. To meet this requirement, a composition of 0·5–0·6%C, 1%Cr, ½%Mo–B

would be suitable. There is scope for further development work to determine the composition giving the best combination of strength, ductility, and impact resistance.

6. The mechanism of bainite formation is the same in these higher carbon steels as previously described for low-carbon steels. In the upper bainite transformation range carbon can diffuse away from the growing bainitic ferrite plates and forms as carbide films at the interface between adjacent plates. At the higher carbon contents carbide can precipitate directly from the austenite but, in either case, the structure consists of an aggregate of bainitic ferrite and carbide, with an increasing amount of carbide as the carbon content increases. In the lower bainite transformation range the carbon cannot diffuse away from the bainitic plate and transformation proceeds by carbon precipitating within the ferrite, with an orientation relationship similar to that between carbide and ferrite in twinned martensite.

7. The reasons put forward for the strength of bainite are:
   (i) fine bainitic ferrite grain size
   (ii) dispersion hardening by precipitated carbides
   (iii) internal stress
   (iv) dislocation density of bainitic ferrite
   (v) solution hardening effect of carbon in solid solution in ferrite.

ACKNOWLEDGMENT

The authors would like to thank Dr F. H. Saniter, O.B.E., Director of Research, The United Steel Companies Ltd, for permission to publish this paper.

REFERENCES

1. K. J. Irvine *et al.: JISI*, 1957, **186,** 54–67.
2. K. J. Irvine and F. B. Pickering: *ibid.*, 1957, **187,** 292–309.
3. K. J. Irvine and F. B. Pickering: *ibid.*, 1958, **188,** 101–112.
4. K. J. Irvine and F. B. Pickering: *ibid.*, 1960, **194,** 137–153.
5. F. B. Pickering: Proc. 4th Int. Conf. Elec. Mic., Vol.1, Berlin 1958, 628.
6. K. J. Irvine and F. B. Pickering: *JISI*, 1963, **201,** 518–531.
7. R. A. Grange and J. M. Garvey: *Trans. ASM*, 1946, **37,** 136.
8. S. V. Radcliffe and E. C. Rollason: *JISI*, 1959, **191,** 56–65.
9. J. Barford and W. S. Owen: *ibid.*, 1961, **197,** 146–151.
10. W. Pitsch and A. Schrader: *Arch. Eisenh.*, 1958, **29,** 485.
11. D. Vasudevan *et al.: JISI*, 1958, **190,** 386–391.
12. J. S. White and W. S. Owen: *ibid.*, 1960, **195,** 79–82.
13. A. E. Austin and C. M. Schwartz: *Proc. ASTM*, 1952, **52,** 543.
14. E. J. Janitsky and M. Baeyertz: 'Metals Handbook', 515–518; 1939.
15. W. Steven and A. G. Haynes: *JISI*, 1956, **183,** 349–359.

Morphology of bainite

D. N. Shackleton and P. M. Kelly

SYNOPSIS

Transmission electron microscopy has been used to study the morphology of bainite formed isothermally in ½%Mo–B steels of various carbon contents. Two principal structures have been identified and the previously reported differences between these two structures have been verified. The transition from upper bainite to lower bainite occurred in the temperature range 300°–400°C. Two types of upper bainite have been observed. In low-carbon steels transformed at high temperatures (near 500°C) the upper bainite consisted of cementite precipitates at the boundaries of the ferrite laths. At lower transformation temperatures (near 400°C) in low-carbon steels and throughout the entire upper bainite transformation temperatures in high-carbon steels, the ferrite in the upper bainite was coarser and the cementite precipitated within the ferrite regions, as well as the boundaries. Lower bainite in all the steels resembled tempered internally twinned martensite. Possible transformation mechanisms for upper bainite and lower bainite have been based on these observed morphological features, in conjunction with a knowledge of the crystallography of cementite in bainite. 2638

INTRODUCTION

THE INABILITY to resolve detailed features of the structure of bainite with the light microscope hampered the early metallographic examinations and it was not until electron microscope techniques became available that progress in this field was achieved.[1-9] Using replica and thin-foil techniques a resemblance in morphology was observed between the bainite formed by isothermal transformation in the lower part of the bainite range (lower bainite) and the tempered martensite in a high-carbon steel, and between the bainite formed in the upper portion of the transformation range (upper bainite) and the tempered martensite in a low-carbon steel.[1,2,3,9] In the lower bainite structure the ferrite is acicular and the cementite is formed within this ferrite at an angle of about 55–65° to the long direction of the ferrite plate.[1-6,9] In upper bainite the ferrite is lath or needle-like in shape and the cementite lies parallel to the needles.[1-6,9] A certain coarsening of the ferrite in upper bainite structures occurs as the transformation temperature is lowered but the cementite is unaltered in its orientation with respect to the ferrite. Although this classification may act as a general guide for the interpretation of these structures, it does not provide a satisfactory criterion, since it is not always possible to distinguish between the two types of bainite by visual examination alone.

In recent years there has been a trend towards a more extensive use of kinetic methods for studying the bainite reaction.[10-13] This work has shown that at about 350°C there is a sharp change in the activation energy in all the steels examined. This change in activation energy is associated with the transition from the lower to the upper bainite structure and can be used as a criterion for differentiating between the two structures.

On the basis of the kinetic and morphological evidence it is not unreasonable to suppose that crystallographic differences may also exist between the two bainite structures. An investigation of the orientation relationships between the ferrite and austenite in bainite was made by Smith and Mehl using X-ray pole figure techniques.[14] They found that bainite formed at 350°C and above exhibited the Nishiyama orientation relationship,[15] while that formed below 350°C obeyed the Kurdjumov–Sachs relation.[16] Since both these relationships are associated with the martensite transformation, these observations indicated a similarity between the formation of bainite and the formation of martensite. Support for this idea increased when it was shown that bainitic ferrite forms by shear.[17-18]

The object of the present work has been to examine the bainite reaction using transmission electron microscopy. The results of this research may be conveniently divided into two sections, the crystallography and the morphology of the transformation, respectively. The crystallographic data will be reported in detail elsewhere[19] and in this paper only the results of the morphological examinations will be described, although in the discussion the observed morphology of bainite will be considered in conjunction with the crystallographic evidence.

EXPERIMENTAL

The transformation to bainite was carried out in steels containing a ½%Mo–B base and varying amounts of carbon. These steels were selected because isothermal transformation to bainite

Dr Shackleton is with the British Welding Research Association, Abington Hall, Cambridge, and Dr Kelly is with the Department of Metallurgy, University of Leeds. (MG/Conf/82/65). UDC No. 669.15′28′781–194:669.112.227.333.

could be carried out over a much wider temperature range than in plain carbon steels. The analyses of the steels and their estimated M_S temperatures are listed in Table I.

Sheet specimens 4× 2½ cm and 350 μm thick were prepared by cold rolling and then austenitized at 1000°C for 3 h in an argon atmosphere. Transformation to bainite was achieved by transferring the specimens to a salt bath held at constant temperature in the sub-critical range. The transformation temperatures selected were 250°C, 350°C, 420°C, or in the range 480°–500°C, and the specimens were held at temperature to produce a fully bainitic structure.

Thin foils suitable for examination in the electron microscope were prepared from the heat treated specimens by chemical thinning and electropolishing.[20] These were examined in a Siemens Elmiskop 1 electron microscope operating at a potential of 100 kV.

RESULTS

The classic needle-like structure associated with upper bainite was only observed a few times in these ½%Mo–B steels, although many examples of the normal low-temperature structure were obtained.

The carbide phase in the bainite was identified (by means of electron diffraction) as cementite, although two regions where $M_{23}C_6$ and M_7C_3 had formed were also observed. As no other carbide was found it was concluded that, apart from exceptional cases, cementite was the bainitic carbide formed in these steels.

The structures developed in the steels by isothermal transformation depended critically upon the temperature at which the transformation was carried out. Marked differences occurred in the shape of the ferrite and the orientation of the cementite when the transformations were made at temperatures above and below 350°C. These differences in the bainite structure are reported below in terms of the temperature at which the isothermal transformation was carried out.

Isothermal transformation at 250°C

In only two of the ½%Mo–B steels was the M_S temperature sufficiently low to enable bainite to be formed at 250°C without producing martensite. These were the steels RM 3870 and RM 3871, containing 0·78% and 0·98%C, respectively.

When the structures formed in these two steels were examined by transmission electron microscopy they were found to be acicular. In general the bainitic ferrite has the appearance of laths or plates, within which the cementite was precipitated as discrete particles. In each ferrite plate the cementite particles

TABLE I Composition of steels used

Steel no.	C, %	Mn, %	Si, %	Cr, %	Mo, %	B, %	Estimated M_S temperature, °C
RM 3866	0·10	0·48	0·42	1·23	0·51	0·002	455
RM 3867	0·20	0·54	0·46	1·07	0·54	0·002	390
RM 3868	0·39	0·56	0·40	1·11	0·52	0·002	310
RM 3869	0·58	0·58	0·38	1·08	0·53	0·002	250
RM 3870	0·78	0·59	0·41	1·08	0·53	0·002	185
RM 3871	0·96	0·63	0·38	1·10	0·51	0·002	135

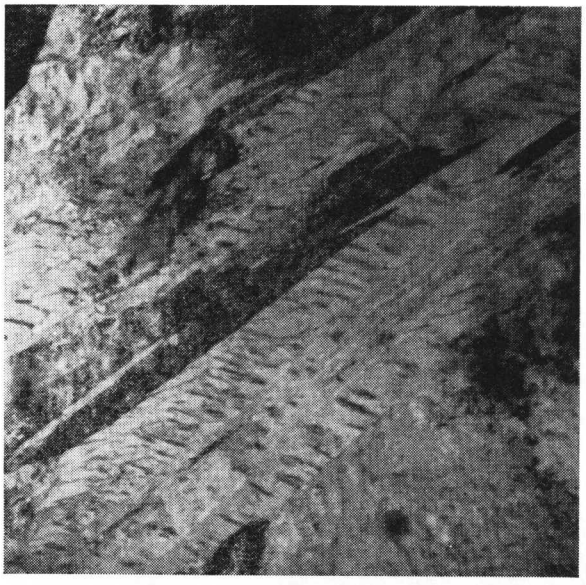

1 *Lower bainite formed at 250°C in the 0·96%C steel* ×30000

were rod-like and lay in the same direction. Ocaasionally the cementite rods were arranged in parallel rows, each particle being oriented across the plate at an angle of about 55–65° to the long direction of the ferrite plate. Such a structure is illustrated in Figure 1 where the cementite (dark) lies within the ferrite plates (predominantly light) in the form of short straight rods that extend up to the ferrite boundaries. Comparison of this structure with previous replica work confirms that it is lower bainite.

Frequently the structures observed at this transformation temperature did not conform to the type of morphology illustrated in Figure 1. In many cases the appearance was of the

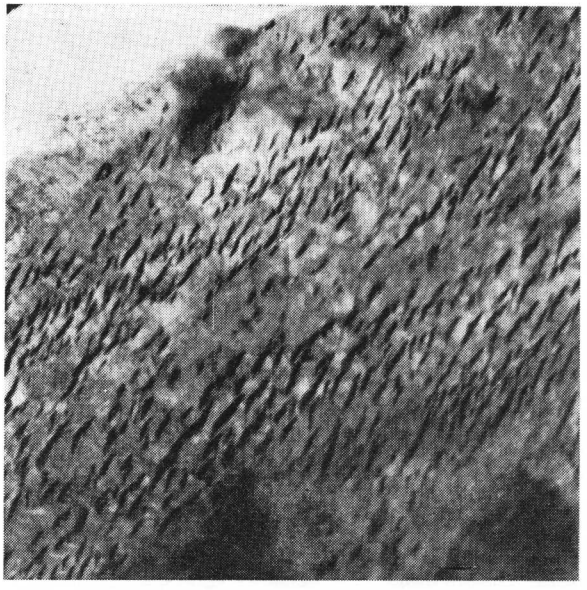

2 *Lower bainite formed at 250°C in the 0·96%C steel* ×30000

3 *Lower bainite formed at 350°C in the 0·58%C steel* ×30000

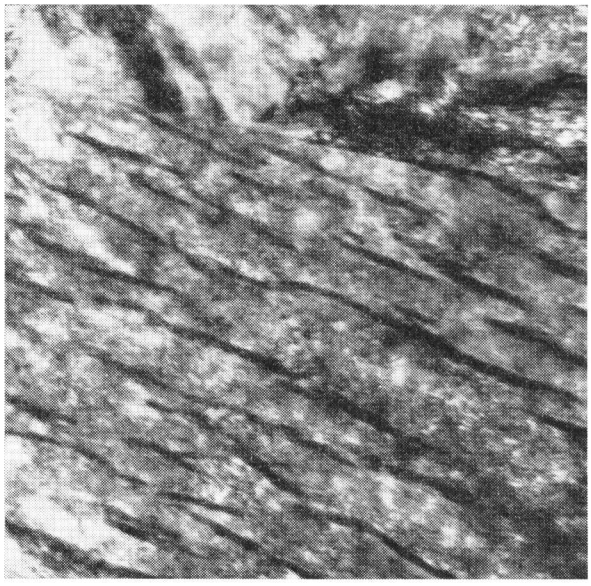

5 *Upper bainite formed at 350°C in the 0·96%C steel* ×60000

type shown in Figure 2 where extensive regions of ferrite were formed, each region containing many parallel cementite particles. Such structures were also encountered adjacent to the classical lower bainite structures shown in Figure 1. It would thus appear that both structures are analogous, the differences depending on the manner in which the plane of the foil cuts the bainite plate.

Isothermal transformation at 350°C

When the isothermal temperature was raised to 350°C the structures that were developed proved in many cases difficult to classify. A number of these structures could be identified as lower bainite although many exhibited morphologies unlike any of those encountered at the lower temperature. The structures that were identified as lower bainite are shown in Figures 3 and 4. The former shows the typical lower bainite structure, whereas the latter is an example of the alternative structure in which the cementite particles are parallel over a large region of ferrite.

Structures other than those shown in Figures 3 and 4 were also observed. In these cases the cementite particles were longer and directed along, rather than at an angle to, the boundaries of the ferrite regions. Such a structure is illustrated in Figure 5 and was later identified as upper bainite. A further example of this

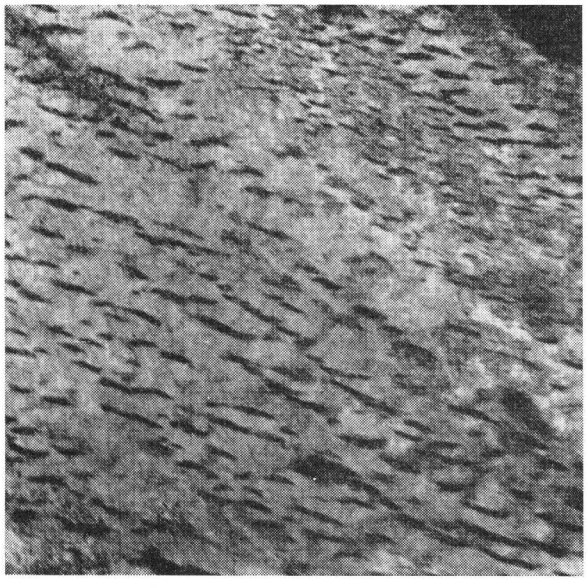

4 *Lower bainite formed at 350°C in the 0·78%C steel* ×30000

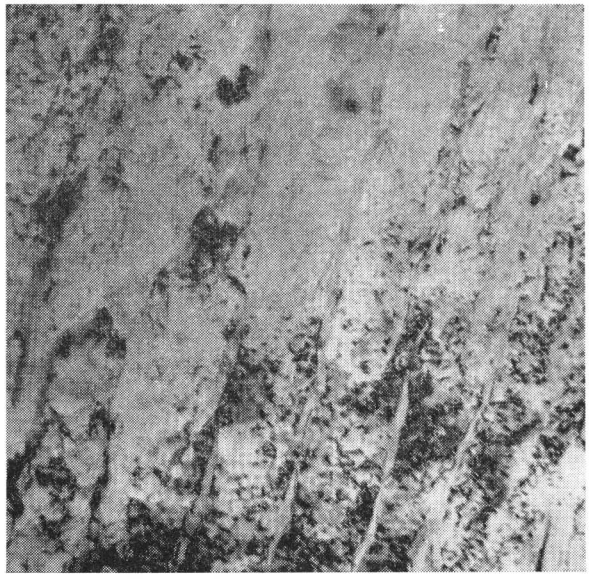

6 *Upper bainite formed at 350°C in the 0·96%C steel* ×60000

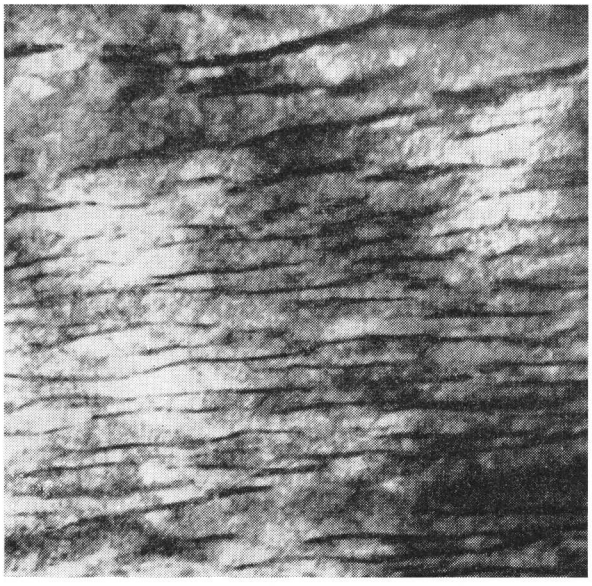

7 *Upper bainite formed at 420°C in the 0·96%C steel* ×30000

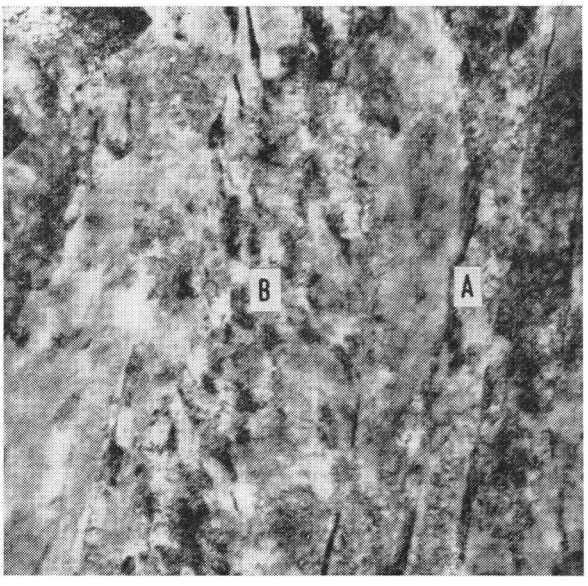

9 *Upper bainite formed at 420°C in the 0·58%C steel* ×30000

structure is shown in Figure 6. This micrograph was taken from an extensive region of ferrite containing long stringers of carbide that were identified as M_7C_3.

In view of the fact that both upper and lower bainite were observed at this transformation temperature the transition between these two structures must occur in the vicinity of 350°C. This is consistent with the results of kinetic studies, where in the particular steels examined the transition occurs at or about this temperature.

Isothermal transformation at 420°C

At this transformation temperature the structures produced showed very little similarity to those resulting from transformation at 250°C. In general the ferrite regions were coarser than in the lower bainite structure and the cementite was directed along, rather than across, the ferrite areas. In the high-carbon steels the cementite always lay within the ferrite regions, but at lower carbon contents there was an increasing tendency for ferrite needles to form with the cementite at the needle boundaries. By comparison with previous work these structures were identified as upper bainite, although this classification was complicated by the variety of cementite–ferrite aggregates observed. In general the structures developed at this transformation temperature consisted of extensive colonies of similarly aligned cementite particles contained within a single ferrite region or extending over several ferrite

8 *Upper bainite formed at 420°C in the 0·96%C steel* ×30000

10 *Upper bainite formed at 420°C in the 0·58%C steel* ×30000

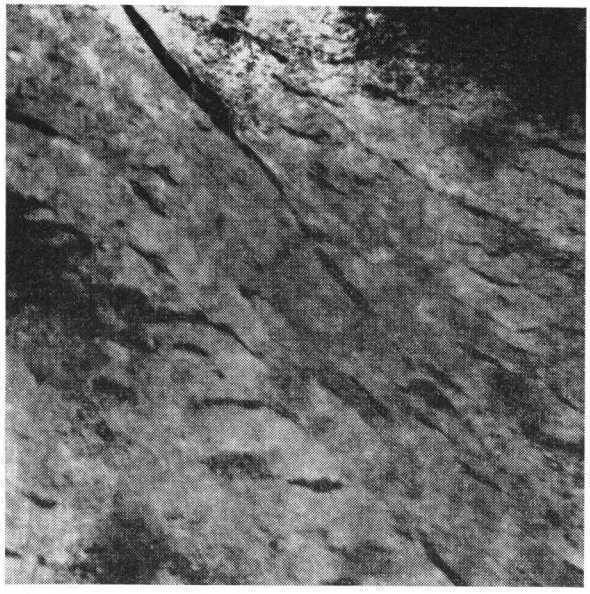

11 *Upper bainite formed at 420°C in the 0·39%C steel* ×30000

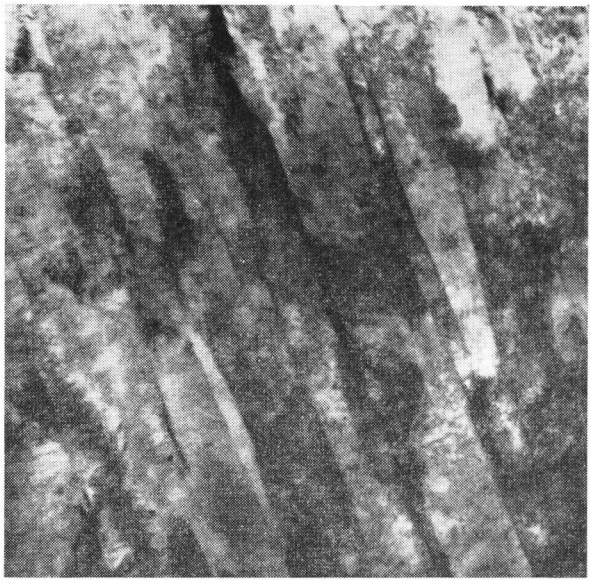

13 *Upper bainite formed at 480°C in the 0·39%C steel* ×30000

crystals. The classical upper bainite structure with the cementite parallel to the ferrite grain boundaries was occasionally observed (Figure 7), although in most cases more than one cementite colony was present within each ferrite region (Figure 8).

The effect of carbon content on the microstructure of the bainite was slight. Apart from differences in the amount of carbide present the most noticeable effect was the greater tendency in the low-carbon steels for ferrite needles to form with the cementite along the needle boundaries. An example of this structure in the 0·6%C steel is shown at *A* in Figure 9. In this micrograph there is a second region of cementite precipitation (*B*) where the carbide appears as dark, irregular, diffuse lumps. This type of structure also occurred in more extensive regions (Figure 10), when it was extremely difficult to distinguish from lower bainite. However, since the classic lower bainite structure illustrated in Figure 1 was not observed in any of the steels examined, it was concluded that this structure (Figure 10) could be classified as upper bainite.

It was possible to form bainite in the 0·4%C steel at 420°C. The structures developed were very similar to those of the higher carbon steels although the tendency towards the needle-ferrite structure was more pronounced. In addition many of the structures (Figures 11 and 12) were more irregular than in the higher carbon steels although they were still recognizable as upper bainite.

12 *Upper bainite formed at 420°C in the 0·39%C steel* ×60000

14 *Upper bainite formed at 480°C in the 0·39%C steel* ×30000

Transformations in the range 480°–500°C

Pickering[6] has shown that the tendency to form the needle-like, upper bainitic ferrite structure (occasionally found in the lower carbon steels transformed at 420°C) becomes more pronounced as the transformation temperature is raised.[6] Using steels similar to those used in this investigation he observed that on raising the transformation temperature there was a transition from the coarse ferrite regions to the needle-like structure and a change in the distribution of the cementite particles.[6] In the low-temperature, coarse bainite structure (called lower bainite by Pickering) the cementite lay within the ferrite regions, while in the high-temperature, needle bainite (called upper bainite by Pickering) the cementite was formed at the ferrite boundaries, parallel to the long dimension of the ferrite needles. In an attempt to detect this transition in the steels used in this investigation, transformations were carried out just below the onset of the pearlite reaction in the temperature range 480°–500°C. On examination it was found that the structures observed depended critically upon the carbon content of the steels. Whereas in the high-carbon steels there was little difference between the structures formed at 420°C and those formed at 480°–500°C, in the lower carbon steels the structure became predominantly needle-like in appearance at the higher transformation temperature and in only a few instances was the coarser bainitic structure observed. The cementite orientation in the low-carbon steels was in many instances similar to that observed by Pickering in that it lay in the ferrite boundaries, parallel to the ferrite needles (Figure 13). However, besides these, a number of structures were observed in which the bainite showed a definite resemblance to lower bainite (Figure 14), although the structures were still upper bainite.

Partial transformation to upper and lower bainite

Partial transformation to bainite was carried out at 420° and 250°C to examine the early stages of both upper and lower bainite formation. These partially transformed materials were examined at various degrees of transformation from 1% to greater than 50%. In all cases the structures observed consisted of the particular bainite formed at that temperature together with martensite.

No ϵ-carbide was detected in the very early stages of transformation, but mixtures of bainite and martensite were occasionally encountered within the same prior austenite grain.

DISCUSSION

Identification of upper and lower bainite

The appearance of the bainite formed by isothermal transformation in the $\frac{1}{2}$%Mo–B steels has been shown in the present work to change considerably as the transformation temperature is raised through the bainite range. In the high-carbon steels where the M_S temperature was depressed sufficiently by the carbon the structure formed by isothermal transformation at temperatures below 350°C was lower bainite. As the transformation temperature was raised a change in the structure occurred and at temperatures above 350°C the upper bainite structure was formed. It is significant, but not necessarily of fundamental importance, that this transition in structure should occur in the $\frac{1}{2}$%Mo–B steels within a similar temperature interval to that detected for other low-alloy and plain carbon steels, since the effect of alloying additions upon the individual *C* curves of the TTT diagrams differ quite markedly. It can only be concluded that, although the positions of the *C* curves are altered, in the steels so far examined the upper and lower bainite *C* curves are affected in such a way as to maintain the transition at approximately the same temperature.

The interpretation of the structures reported in the previous section implied a degree of confidence that could not have been achieved by means of a purely morphological examination. Despite the fact that a number of the micrographs could be identified with ease as upper or lower bainite, many of the structures were more complex and could not be classified according to the orientation and distribution of the cementite particles. In the preliminary investigations carried out identification was based on the 350°C transition determined in kinetic investigations. This later proved unacceptable, since, firstly, it had not been established that this criterion was applicable to the $\frac{1}{2}$%Mo–B steels and, secondly, where this transition had been observed it had not been correlated with the structures formed above and below the transition temperature. This difficulty was overcome, however, as a result of the determinations of the crystallographic features of the bainite structures. As thin foils were being examined in transmission, electron diffraction could be carried out and the crystallographic features of the matrix and precipitate phases analysed. This enabled the orientation relationships and habits of the cementite–ferrite aggregates to be determined and revealed differences between the structures formed above and below 350°C, which could be associated with the upper and lower bainite structures. These differences are reported in detail elsewhere[19] and will only be summarized here.

In the lower bainite structures formed below 350°C the orientation relationship between cementite and ferrite was:

$$\begin{aligned}&(001)_{Fe_3C} \parallel (211)_\alpha\\ &[100]_{Fe_3C} \parallel [0\bar{1}1]_\alpha\\ &[010]_{Fe_3C} \parallel [1\bar{1}\bar{1}]_\alpha\end{aligned} \quad \ldots\ldots\ldots\ldots\ldots\ldots\ldots\ldots\ldots\ldots \quad (1)$$

This relationship is the same as that previously observed between cementite and ferrite during the tempering of martensite.[21–25] In the tempering of martensite a second relationship is also obeyed, although it is less frequent than the one given above.[23] This second orientation relationship, i.e.

$$\begin{aligned}&(001)_{Fe_3C} \parallel (\bar{2}\bar{1}5)_\alpha\\ &[100]_{Fe_3C} \text{ within } 2{\cdot}6^\circ \text{ of } [3\bar{1}1]_\alpha\\ &[010]_{Fe_3C} \text{ within } 2{\cdot}6^\circ \text{ of } [131]_\alpha\end{aligned} \quad \ldots\ldots\ldots\ldots\ldots\ldots\ldots\ldots\ldots\ldots (2)$$

was also detected in lower bainite but its occurrence was extremely rare.

When the transformation temperature was raised to 350°C, where upper and lower bainite both formed, the orientation relationships between cementite and ferrite changed. The predominant relationship remained the same as that found at the lower temperature (i.e. relationship (1)), but the second relationship found at the lower temperature was not observed. Instead a number of new relations were found and these differed considerably from the two given above.

On raising the transformation temperature to 420°C the orientation relationships that were obeyed showed no material difference from those determined at 350°C, although the new

relationships became more frequent. These were found to occur in the ratio of one new relationship for every two of type (1). In all, 36 diffraction patterns were analysed for bainite formed at 420°C; 23 of these were consistent with relationship (1) and the remaining 13 with one of the new relationships. Although considerable variation existed between these alternative new relationships, it was found that, together with (1), they could all be produced by relating the cementite and the ferrite to the common parent phase austenite. Basically this was done by relating the cementite to the austenite using the Pitsch austenite–cementite relationship[26,27]

$$\begin{aligned}(001)_{Fe_3C} &\parallel (\bar{2}25)_\gamma \\ [100]_{Fe_3C} &\parallel [\bar{5}5\bar{4}]_\gamma \\ [010]_{Fe_3C} &\parallel [\bar{1}\bar{1}0]_\gamma\end{aligned} \quad \ldots\ldots(3)$$

The austenite was then considered to have transformed to ferrite following a variant of the Kurdjumov–Sachs orientation relationship[16]

$$\begin{aligned}(111)_\gamma &\parallel (101)_\alpha \\ [1\bar{1}0]_\gamma &\parallel [11\bar{1}]_\alpha\end{aligned} \quad \ldots\ldots(4)$$

By relating the cementite to austenite by the same variant of (3) above and then using different variants of (4) to relate the austenite and ferrite, it is possible to derive 12 different ferrite–cementite orientation relationships. Two of these are close to relationship (1) while the other ten differ from each other and from (1). When this procedure was adopted all the new alternative cementite–ferrite relationships found at 350°C and above could be accounted for.

This means that all the relationships observed in what the kinetic results would term the 'upper bainite range' can be explained if the ferrite and the cementite are related through the parent phase austenite. There is no need to use this argument for bainite formed below 350°C, where the observed orientation relationships are all explicable in terms of the precipitation of cementite in ferrite. These differences in orientation relationships above and below 350°C provide a powerful means of distinguishing between upper and lower bainite even when the structures appear morphologically similar and were used to a large extent to classify the structures described previously.

Comparison of bainite with martensite

It is generally recognized that the structures formed during the bainite transformation are very similar to those developed when martensite is tempered, although the exact details are not yet clearly understood.[1–3,9] This identification of bainite with tempered martensite arose from the observation that the morphology of lower bainite was very similar to tempered high-carbon martensite and the upper bainite structure was not unlike that found in a low-carbon steel transformed to martensite and tempered at 400°C. It is significant that this similarity is more pronounced in the case of lower bainite, where both the cementite and the ferrite can be compared with the tempered martensite structure, while in upper bainite only the ferrite bears any direct resemblance to the tempered martensite structure. Besides these morphological features common to both structures, other investigations have revealed further similarities. Smith and Mehl showed that the two austenite–ferrite relationships obeyed by upper and lower bainite were associated with martensite transformation, and they therefore concluded that the mechanisms of bainite and martensite formation were alike.[14] More striking evidence for a martensitic-type transformation of the bainitic ferrite has been reported by Ko and Cottrell, who detected surface markings on a polished surface associated with the transformation of austenite to bainite.[17,18] These surface tilts indicate the propagation of a coherent or martensitic interface but they do not necessarily infer a truly martensite transformation since, as Christian pointed out, a true martensitic transformation is diffusionless.[28] Thus, although the formation of bainitic ferrite may well be a shear reaction it is not strictly martensitic in the sense of being a diffusionless transformation.

The bainite structures observed in the present investigation are only in partial agreement with the findings of previous metallographic examinations. While the lower bainite resembled the corresponding tempered twinned martensite structure, in the upper bainite range the only similarity with tempered martensite was the needle-like bainitic ferrite formed at high temperatures in the low-carbon steels. No valid comparison could be made between the tempered martensite structures and the upper bainite structures formed in the higher carbon steels.

In view of these morphological differences between the upper bainite and tempered martensite structures it would be expected that equivalent differences would be encountered in the crystallography of these structures. The determinations of orientation relationships revealed that the upper bainite structure did differ from tempered martensite, while no difference existed between lower bainite and tempered high-carbon martensite. While the predominant orientation relationship between cementite and ferrite in both bainite structures was the same as the predominant tempering relationship (i.e. relationship (1)), only in the case of lower bainite were the alternative relationships in agreement with those found in tempered martensite. Furthermore, the habit plane and long direction of the cementite particles were only similar to the tempered martensite structure in the case of the lower bainite structure. In these structures the cementite habit plane was found to lie in a region containing $\{110\}_\alpha$ and $\{112\}_\alpha$, while the habit direction was approximately $<111>_\alpha$. This is consistent with the determinations of habit planes and directions for cementite precipitation during the tempering of martensite.[24,25] The habit plane of the cementite particles in upper bainite was found to be $(101)_{Fe_3C}$ and the long direction $[010]_{Fe_3C}$, both in terms of the cementite lattice. These results applied irrespective of the orientation relationship obeyed between the cementite and ferrite. When relationship (1) was obeyed these habits were associated with $\{211\}_\alpha$ and $<111>_\alpha$ respectively, but with the alternative relationships no consistent habits in terms of the ferrite lattice were obtained. Although the $\{211\}_\alpha$ habit found in conjunction with relationship (1) also occurs in tempered martensite, this habit plane only applies to cementite formation along the boundaries of the twins within the martensite plates. In the absence of twins the cementite forms with a Widmanstätten structure with a habit plane $(110)_\alpha$ (or $(100)_{Fe_3C}$). Hence, for the precipitation of cementite in upper bainite to occur by a similar process to that in tempered martensite the presence of internal twins would be required. In the type of martensite normally associated with upper bainite such twins do not occur.

From the above discussion it is apparent that there is a close resemblance between lower bainite and tempered martensite. This would suggest that the sequence of formation is the same in both structures. It is also apparent that, although certain features of the upper bainite and tempered martensite structure are alike, there are considerable differences which can only result from different transformation sequences operating in the formation of each structure. Since certain aspects of the transformation sequences for upper and lower bainite may be deduced from the crystallographic data, this will be considered in greater detail below.

Mechanisms of bainite formation

Although several attempts have been made to account for bainite formation most of the explanations put forward have not been adequately correlated with experimental observation. It has been generally recognized that the structural differences between upper and lower bainite result from different mechanisms of formation, but little has been achieved in understanding these mechanisms apart from the detection of certain analogies to the martensite and tempered martensite structures. Because of this lack of data, only a general outline of the mechanisms operating in the bainite transformations has been possible. These were best summarized by Christian[28] who postulated that in lower bainite the carbon may be taken into the ferrite and subsequently precipitated behind the ferrite–austenite interface, while in upper bainite the ferrite grows into the austenite matrix pushing carbon ahead of it until carbide is nucleated in the carbon-enriched regions between the ferrite grains. From the shape changes associated with the transformation Christian further suggested that the crystallography of formation of ferrite in upper bainite should resemble that of martensite in a very low carbon steel, while the appropriate resemblance for lower bainite should be the formation of martensite in the particular steel considered.

The mechanisms presented by Christian define the sequence of events operating in the formation of both bainite structures. However, since they depend upon results obtained from kinetic experiments it is desirable that, before they become universally accepted, the deductions of the kinetic work should be verified. This is achieved by the crystallographic determinations carried out in the course of the present investigation. These results are in agreement with the general features of the mechanisms outlined above and in addition allow the transformation path for the cementite to be specified in both the upper and lower bainite structures. The kinetic work and the determination of ferrite–cementite orientation relationships mentioned above lead to the conclusion that in lower bainite the cementite precipitates in the supersaturated ferrite and *not* in the austenite. This implies the following transformation sequence for lower bainite formation. In a particular region of austenite a ferrite plate is formed martensitically. This region of ferrite (or martensite) will have approximately the same carbon content as the matrix, and soon after formation the carbon will precipitate as cementite along the twin boundaries of the martensite. The carbon content of the surrounding austenite could then be reduced by carbon diffusing into the ferrite (probably along the twin boundaries) to increase the size of the cementite particles. This will mean that the M_S temperature of the surrounding austenite is raised and a further shear transformation will occur to form more supersaturated ferrite. This procedure will be repeated until some structural inhomogeneity (or the lack of any untransformed austenite) halts the growth of the bainite plate. Admittedly there is no conclusive direct evidence from the present work to demonstrate the presence of internal twins in lower bainite. However, it is known that during tempering the twins are removed by the precipitation of cementite.[25] Further, the habit planes and orientation relationships of the cementite in lower bainite are consistent with precipitation on twins.

In upper bainite formation the kinetic data imply that the rate-controlling step is the diffusion of carbon in austenite. The orientation relationships determined in the course of the present work can only be explained for upper bainite if the ferrite and the cementite are related through their common parent austenite. The conclusion to be drawn from this is that the cementite and the ferrite nucleate independently in austenite. There is no way of using this crystallographic data to decide whether cementite nucleates before ferrite or vice versa, but the formation of cementite in ferrite rather than in austenite is definitely ruled out in a number of the cases analysed. The kinetic and crystallographic data are therefore in agreement and lead to the following transformation mechanism for upper bainite. Cementite is nucleated in the austenite depleting the surrounding region of carbon and allowing transformation to ferrite. Alternatively, following the possibility that ferrite is formed first, this ferrite can only grow by rejection of carbon ahead of the advancing ferrite–austenite interface. This rejection of carbon will be achieved by forming cementite in the austenite ahead of the growing bainite–ferrite interface.

The habit plane and direction determinations for cementite in upper bainite support the idea of independent nucleation of ferrite and cementite in upper bainite. If the alternative orientation relationships found in upper bainite were *not* due to independent formation of the two phases in austenite the habit plane and directions should differ from one relationship to the other. This is not the case and in fact the morphology of the cementite in upper bainite is always the same irrespective of the orientation relationship to the ferrite and is identical to the morphology of proeutectoid cementite precipitation in austenite, i.e. the habit plane is always $(101)_{Fe_3C}$ and the long direction $[010]_{Fe_3C}$.[27] Consequently it can only be concluded that in upper bainite the cementite and the ferrite are in fact both formed separately in the austenite.

Completely independent nucleation of cementite and ferrite in the austenite does not always occur since, if this were so, a random distribution of the alternative relationships would be expected. In fact the tempering relationship (1) was obeyed in two out of every three diffraction patterns analysed. Consequently the second phase to nucleate in the austenite is not always completely independent of the first but most probably forms adjacent to it. This result is not entirely surprising as the nucleation of ferrite immediately adjacent to cementite (or vice versa) is to be expected.

The change in ferrite structure from the needle to the coarse form, within the upper bainite transformation range, cannot be related to any specific temperature since it is strongly dependent upon the composition of the steel. The high-temperature

needle structure is probably formed as a result of ferrite needles entrapping regions of austenite during their growth. At a later stage of the transformation these austenite regions break down, forming cementite in the boundaries of the needles, so producing the familiar feathery structure. At the lower transformation temperatures in the upper bainite range the ferrite which forms retains its acicularity but becomes coarser than that formed at higher temperatures. During the formation of this coarse upper bainite the cementite is probably precipitated in the austenite ahead of the bainite–austenite interface and is then engulfed by the growing ferrite regions, producing the coarse bainite structures containing cementite particles within the ferrite grains.

CONCLUSIONS

The morphology of the cementite–ferrite aggregates formed during isothermal transformation to upper and lower bainite were not the same in the two structures. The transition in structure occurred at about 350°C and the lower bainite structures formed below this temperature were identical to the structure of tempered internally twinned martensitic plates. In the temperature range above 350°C two types of upper bainite structure were formed. When the low-carbon steels were transformed at high transformation temperatures the cementite lay in the boundaries of the ferrite needles. At lower transformation temperatures in the low-carbon steels and throughout the whole of the range in the high-carbon steels the upper bainitic ferrite was coarser and the cementite occurred within the ferrite regions.

It is concluded from a combination of these morphological results and a knowledge of the cementite crystallography in both upper and lower bainite that the mechanisms of formation in both the bainite structures differ considerably. It is proposed that the mechanism operating in the formation of lower bainite is identical to that in the formation and tempering of martensite. Initially, supersaturated ferrite forms from the austenite by a shear process and cementite subsequently precipitates within the ferrite.

At transformation temperatures above 350°C the upper bainite formation differs from that of lower bainite in that the cementite, as well as the ferrite, is nucleated in the austenite. Thus, during transformation, ferrite and cementite both form in the austenite and as growth proceeds the cementite may be engulfed by the advancing ferrite.

ACKNOWLEDGMENTS

This research was carried out in the Department of Metallurgy, The University of Leeds, under the direction of Professor J. Nutting, to whom the authors' thanks are due for his interest, encouragement, and advice. One of the authors (D.N.S.) acknowledges with gratitude the provision of a DSIR maintenance award which enabled this work to be carried out. Thanks are also due to The United Steel Companies Ltd for the supply of the steels used in this investigation.

REFERENCES

1. 1st Progress Report of Sub Committee XI, ASTM Committee E-4; *Proc. ASTM*, 1950, **50,** 444.
2. 2nd Progress Report of Sub Committee XI, ASTM Committee E-4: *ibid.*, 1952, **52,** 543.
3. 4th Progress Report of Sub Committee XI, ASTM Committee E-4, *ibid.*, 1954, **54,** 568.
4. L. HABRAKEN: Proc. 4th Int. Conf. on Electron Microscopy, 621; 1958, Berlin.
5. R. M. FISHER: *ibid.*, 579.
6. F. B. PICKERING: *ibid.*, 626.
7. S. MODIN: *Jernkont. Ann.*, 1958, **142,** 37–80.
8. M. ECONOMOPOULOS *et al.*: *Mém. Sci. Rev. Mét.*, 1963, **60,** 11–22.
9. K. SHIMIZU and Z. NISHIYAMA: *Mem. Inst. Sci. Ind. Res. Osaka Univ.*, 1963, **20,** 43.
10. P. VESUDEVAN *et al.*: *JISI*, 1958, **190,** 386–391.
11. S. V. RADCLIFFE and E. C. ROLLASON: *ibid.*, 1959, **191,** 56–65.
12. J. S. WHITE and W. S. OWEN: *ibid.*, 1960, **195,** 79–82.
13. R. H. GOODENOW *et al.*: *Trans. AIME*, 1963, **227,** 651–658.
14. G. V. SMITH and R. F. MEHL: *Trans. AIME*, 1942, **150,** 211.
15. Z. NISHIYAMA: *Sci. Rep. Tohoku Univ.*, 1934–5, **23,** 638.
16. G. V. KURKJUMOV and G. SACHS: *Z. Physik*, 1930, **64,** 325.
17. T. KO and S. A. COTTRELL: *JISI*, 1952, **172,** 307–313.
18. T. KO: *ibid.*, 1953, **175,** 16–18.
19. D. N. SHACKLETON and P. M. KELLY: to be published.
20. D. N. SHACKLETON: Ph.D. Thesis; University of Leeds, 1964.
21. I. V. ISAICHEV: *Zhur. Tekhn. Fiz.*, 1941, **11,** 412.
22. Y. A. BAGARYATSKII: *Doklady AN SSSR*, 1950, **73,** 1161.
23. W. PITSCH and A. SCHARDER: *Arch. Eisenh.*, 1958, **29,** 485.
24. P. M. KELLY and J. NUTTING: *Proc. Roy. Soc.*, 1960, **259,** 45–58; *JISI* 1961, **197,** 199–211.
25. E. TEKIN and P. M. KELLY: Presented at Symposium 'Precipitation from iron base alloys', Ohio, USA, 1963, to be published.
26. W. PITSCH: *Acta Met.*, 1962, **10,** 897–900.
27. W. PITSCH: *Arch. Eisenh.*, 1963, **34,** 381–390.
28. J. W. CHRISTIAN: Symposium on decomposition of austenite by diffusional processes', 371–386; 1962, New York, Interscience.